

1 **Answer to Reviewers Comments for “Structure, dynamics, and trace gases**  
2 **variability within the Asian summer monsoon anticyclone in extreme El Niño**  
3 **of 2015–16” by Ravindra Babu et al.**  
4

5 Dear Editor,  
6 Rolf Müller,  
7

8 We are submitting our revised manuscript titled “Structure, dynamics, and trace gases variability  
9 within the Asian summer monsoon anticyclone in extreme El Niño of 2015–16”. We thank the two  
10 Reviewers for their detailed and well-structured comments, which helped to significantly improve  
11 the manuscript content further. We have made substantial changes to the manuscript in order to  
12 thoroughly address the Reviewers’ suggestions and comments. Main changes include:

- 13 ● As per the reviewer suggestion, we have now reanalyzed the geopotential height and winds  
14 from **NCEP-DOE Reanalysis 2** and replaced **Figures 2 to 4** with updated data in the  
15 revised manuscript.
- 16 ● We have also done a statistical analysis for the trace gases and the tropopause anomalies  
17 and highlighted the anomalies (**star symbols in Figures 7 to 10**) larger than  $\pm 2\sigma$  from  
18 long-term mean.
- 19 ● We have modified the text in the revised manuscript as suggested by the both Reviewers.

20 With these changes, we are convinced that the paper is highly relevant for a wide-ranging journal  
21 like Atmospheric Chemistry and Physics. We have provided our answers point-by-point to both  
22 the reviewer’s comments and suggestions.

23 Reviewer’s comments are in normal black color font, followed by our respective replies in blue  
24 color font.

25 Kind regards,

26 **Saginela Ravindra Babu** (on behalf of the co-authors)  
27  
28  
29  
30  
31  
32  
33  
34

## Replies to Referee #2 Comments/Suggestions

Anonymous Referee #2

This a very interesting and well-structured paper that should be published by ACP. It shows how a strong boreal summer ENSO event like that in 2015 significantly weakens the strength of the Asian summer monsoon anticyclone (ASMA). Typically, ENSO events happen during the boreal winter, so summer events, which are rather rare, may be important in a changing climate. The paper shows how the composition of air within the ASMA around the UTLS is strongly influenced by such a summer El Nino, with less tropospheric (CO, WV) and more stratospheric (ozone) signatures (all these quantities are derived from the MLS observations). Also the warming of the tropopause (lapse rate and cold point) within the ASMA as derived from the COSMIC data is very convincing. Thus, I would like to recommend this paper for publishing in ACP by taking into account the following critical points. There are also few important formulation issues listed in the minor comments.

**Reply: First of all, we wish to thank the reviewer for going through the manuscript carefully, appreciating actual content of the manuscript and offering potential solutions to improve the manuscript content further. We have revised the manuscript while considering both the reviewer's comments/suggestions.**

### Major points

In Figs 6-9, I would recommend to show which differences are statistically significant by comparing the difference with the standard deviation  $\sigma$  of the calculated mean value. Typically, hatched areas (e.g. by black dots) are used to show which differences are larger than  $2\sigma$ .

**Reply: Thanks for the valuable suggestion. As for the reviewer suggestion, we have done a statistical analysis for the obtained anomalies for trace gases and the tropopause temperatures. Further, we compared the obtained anomalies with the  $\pm 2\sigma$  standard deviation of background long term mean. We have highlighted the values which are greater than the  $\pm 2\sigma$  standard deviation in Figures 7 to 10 in the revised manuscript.**

### Minor comments:

Abstract, P1 L13

In your abstract, you talk about the extreme El Nino 2015-16 event, so my impression was that you will discuss the winter part of this event...however your topic is much more the unusual summer start of this event...maybe you should reformulate your abstract, maybe something like this:

A weak 2014/15 El Nino developed in 2015 to a strong boreal summer event which continued and even enhanced during the following winter. In this work, the detailed changes in the structure, dynamics and trace gases within the Asian summer monsoon anticyclone (ASMA) is delineated by using Aura Microwave Limb Sounder (MLS) measurements, COSMIC Radio Occultation (RO) temperature, and NCEP reanalysis products. Our analysis concentrates only on the summer months of July and August 2015 when Nino3.4 index started to exceed 1.5 values. The results show that the ASMA structure was quite different in summer 2015 as compared....

**Reply: Authors thanks to the reviewer for a nice suggestion. We have modified the abstract in the revised manuscript as suggested by the reviewer.**

Abstract, P2 L29-31

81 ...and further supports...

82 During a “normal” El Niño which typically maximizes during the boreal winter, there is a shift of  
83 convection from the Western to the Eastern Pacific, so something similar has to be expected for  
84 the summer El Niño...so this is for me one of the main reasons for the warming of the tropopause  
85 in the ASM region. Of course, changes in ozone you recognized follow this shift in convective  
86 patterns and also influence the tropopause temperature...

87 **Reply: Yes. The well-known Walker circulation reversal during the El Niño events suppresses**  
88 **the convection over the ASM region. We agree with the reviewer that shift in the convection**  
89 **during El Niño is also one of the plausible reasons for the observed tropopause warming in**  
90 **2015. The enhanced ozone (heating due to O<sub>3</sub>) alone might be not the reason for the**  
91 **tropopause warming. Apart from ENSO induced convection, other factors also can influence**  
92 **the tropopause temperature, such as stratospheric QBO, and atmospheric waves. We have**  
93 **discussed these things in the results section in the revised manuscript.**  
94 **However, to avoid confusion, we have removed this sentence from the abstract in the revised**  
95 **manuscript.**

96

97 P2 L36  
98 boreal summer, centered at 25N and extending....

99 **Reply: Corrected as per suggestion.**

100

101 P2 L42  
102 Santee et al., 2017).

103 **Reply: Corrected as per suggestion.**

104

105 P2 64  
106 ....Das and Suneeth, 2020). Most of the water vapor enters the stratosphere through....

107 P2 68-71  
108 ....about the causative mechanism...???

109 ....is mainly controlled by the advection and tropopause altitude...

110 I think that the cold point tropopause mainly dominates the WV concentrations in the lower  
111 stratosphere. I would recommend to reformulate all statements related to Das and Suneeth  
112 publication.

113 **Reply: We have reformulated all statements related to ‘Das and Suneeth publication’ in the**  
114 **revised manuscript.**  
115 **We have revised the sentences as follows:**  
116 **‘Recently, Das and Suneeth (2020) reported about the distributions of WV in the UTLS over**  
117 **the ASMA during summer using thirteen years of Aura Microwave Limb Sounder**  
118 **observations. They concluded that WV in the UTLS region inside the central part of ASMA**  
119 **is mostly controlled by horizontal advection and very less from the local process and**  
120 **tropopause temperature in both summer and winter’.**

121

122 P4 L78-105, Tweedy et al., 2018 versus Yan et al., 2018  
123 Maybe you should make more clear, even in the introduction, how to classify the 2015-2016 El  
124 Niño event: In my understanding there was a weak El Niño during the 2014/15 boreal winter which  
125 developed to strong boreal summer ENSO event (following the definition discussed in Tweedy et  
126 al., 2018). This summer ENSO event continued and even enhanced until the winter 2015/16. Thus,

127 following the definition given in Yan et al., 2018, it was a long-lasting El Niño event because it  
128 lasted over two consecutive winters.

129 **Reply: Thanks for the suggestion. We have modified the text as suggested.**

130 **We have revised the sentences as follows:**

131 **'It was started as a weak El Niño during 2014-15 boreal winter and it developed as a strong**  
132 **boreal summer El Niño event in 2015 (Tweedy et al., 2018). Further, this strong boreal**  
133 **summer event continued and significantly enhanced until the boreal winter of 2015-16'.**

134

135 P8 L180

136 In a similar manner, we...

137 **Reply: Corrected in the revised manuscript.**

138

139 P10 L194-195

140 ...in August if compared to July.

141 **Reply: Corrected in the revised manuscript.**

142

143 P10 L195

144 ...over the northwestern Pacific...(see also L406)

145 **Reply: Corrected in the revised manuscript.**

146

147 P10 L206

148 ...as well as at 150 hPa...

149 **Reply: Corrected in the revised manuscript.**

150

151 P12 L232

152 ...of the westerlies.

153 **Reply: Corrected in the revised manuscript.**

154

155 P12 L242

156 Western Pacific (use large letters for geographic names)

157 **Reply: Corrected in the revised manuscript.**

158

159 P14 Figure 5, caption

160 please write correctly the PV units.

161 **Reply: Corrected in the revised manuscript.**

162

163 P15 L277

164 ...penetration...has started

165 **Reply: Corrected in the revised manuscript.**

166

167 Figure 6 and Figure 7, captions please mention that PV is from ERA-Interim in Figure 6 and ozone  
168 from MLS in Figure 7

169 **Reply: Mentioned in the revised manuscript.**

170

171 General

172 Sometimes you write O3 and sometimes O3....

173 **Reply: We make it consistent throughout the manuscript.**  
174  
175 P16 L289  
176 Further, we quantify the change in O3, CO and WV concentration...within the ASM during 2015  
177 caused by the dynamical effects....and we do not need the last sentence, I think.  
178 **Reply: Modified as per suggestion.**  
179  
180 P16 L295  
181 It is well-documented that the ASMA contains low (high)..  
182 **Reply: Corrected as per suggestion.**  
183  
184 P16 L298  
185 Differences of the trace gases within and outside of the ASMA are attributed to..  
186 **Reply: Corrected in the revised manuscript.**  
187  
188 P16 L301  
189 two times “strongly”  
190 **Reply: Corrected in the revised manuscript.**  
191  
192 P16 L303  
193 ...(Yan et al., 2018...)  
194 **Reply: Corrected in the revised manuscript.**  
195  
196 P17-19 L314-351  
197 There are few repetition in the text...you should also explain the strong negative values in Fig 7  
198 probably related to a stronger upwelling in the BD circulation during this summer El Nino (see  
199 also Diallo et al., 2018). The sentence in L346 does not contain any verb....The sentence in L349-  
200 351 is confusing..  
201 **Reply: We have taken care most of the things in the revised manuscript.**  
202  
203 P20, Figure 8 + text  
204 There is also a considerable year-to-year variability of the CO sources (biomass burning) which  
205 may be also the reason for the CO anomaly in 2015, see e.g. Santee et al., JGR, 2017....maybe you  
206 would like to discuss this point.  
207 **Reply: The authors fully agree with the reviewer that there is a considerable year-to-year**  
208 **variability of the CO sources. Apart from this, a weak vertical transport from the boundary**  
209 **layer to the UTLS region over the ASM region is generally observed during El Niño period**  
210 **(Fadnavis et al., 2019). We have discussed about this in the revised manuscript as suggested**  
211 **by the reviewer.**  
212  
213 P21 Figure 9  
214 There is a significant enhancement of WV in the tropics, probably related to warmer tropical  
215 temperatures following EL Nino. For the typical winter El Nino a positive water anomaly is  
216 expected in the tropical tropopause region (see Randel et al. 2009 or Konopka et al., 2016), so  
217 something similar can be expected for a summer El Nino  
218 **Reply: Yes. The authors fully agree with the reviewer that there is a significant enhancement**

219 of WV particularly at 146 hPa in July and 100 hPa in August months. We have discussed  
220 about this in the revised manuscript as suggested by the reviewer.

221  
222 P22 L389  
223 ...we tried to...please reformulate

224 **Reply: Modified in the revised manuscript as suggested.**

225  
226 P22 L395-96  
227 It is well-documented that...are occur (?) This sentence is confusing

228 **Reply: Apologies for confusion. We have modified entire sentence in the revised manuscript.**

229  
230 P22 L401  
231 Kindly noticed...please reformulate

232 **Reply: Modified in the revised manuscript as suggested.**

233  
234 P22 L406  
235 Nortwestern Pacific

236 **Reply: Corrected in the revised manuscript.**

237  
238 P23 L415-416  
239 During winter El Nino, there is a shift of convection from the Western to the Eastern Pacific,  
240 something similar has to be expected for the summer El Nino...so this is for me one of the main  
241 reasons for the warming of the tropopause in the ASM region (less convection). Of course, changes  
242 in ozone you recognized follow this shift in convective patterns and also influence the tropopause  
243 temperature

244 **Reply: We agree with the reviewer that the shift in the convection during El Niño is also one  
245 of the plausible reasons for the observed tropopause warming in 2015. As mentioned earlier,  
246 the enhanced ozone (heating due to O<sub>3</sub>) alone might be not the reasons for the tropopause  
247 warming. Apart from ENSO induced convection, other factors also can influence the  
248 tropopause temperature, such as stratospheric QBO and atmospheric waves. We have  
249 discussed this thing in the results section in the revised manuscript.**

250  
251 P24 438  
252 in the stratospheric tracer (O<sub>3</sub>) within the ASMA..

253 **Reply: Corrected in the revised manuscript as suggested.**

254  
255  
256 **We once again thank the reviewer for going through the manuscript carefully and offering  
257 potential solutions which made us to improve the manuscript content further.**

258  
259 —END—

260  
261  
262  
263  
264

### Replies to Referee #3 Comments/Suggestions

This paper shows the structure, dynamics, and trace gasses changes within the Asian summer monsoon anticyclone (ASMA) in July and August 2015 during extreme El Niño using satellite measurements and NCEP reanalysis data. The spatial extension of the ASMA was quite larger than the mean during 2005-2014 in July and exhibits a strong southward shift. Intense Rossby wave breaking events along the subtropical westerly jet are also appeared in July. For tracers, carbon monoxide (water vapor) decreased by 30% (20%), the ozone increased by 40% at 100 hPa compared to the long-term (2005-2014) mean in July. In August, the ASMA splits into two and western Pacific mode. Additionally, the tropopause temperature displays positive anomalies within the ASMA in 2015.

The topic of this study is interesting and the authors have presented the results with sufficient analyses. However, some statements in the paper are not precise. The manuscript could be considered to be published in ACP after the following revision.

**Reply: First of all, we wish to thank the reviewer for going through the manuscript carefully, appreciating actual content of the manuscript and offering potential solutions to improve the manuscript content further. We have revised the manuscript while considering both the reviewer's comments/suggestions.**

Page2 Line 29-31: The last sentence in the abstract is unclear. Please revise this sentence. In the abstract “the spatial extension of the ASMA shows larger than the long-term mean in all the regions except over northeastern Asia”, and the last sentence in the abstract “Overall, warming of the tropopause region due to the increased O3 weakens the anticyclone”. ... increased ozone weakens the anticyclone?, but the authors mean that the large spatial extension of the ASMA in July 2015 is it contradict?

**Reply: The changes in the O3 concentrations (increase/decrease) within the ASMA are one of the possible mechanisms to strengthening/weakening of the ASMA (Braesicke et al., 2011). By using idealized climate model experiments, Braesicke et al. (2011) clearly demonstrated that the strengthening (weakening) of the ASMA occurred when the O3 is decreased (increased) within the ASMA. The increased O3 within the ASMA warms the entire anticyclone region and weakens the ASMA (Braesicke et al., 2011). Our results from the present study are also in agreement with the results of Braesicke et al. (2011). We also observed a pronounced increase of O3 within the ASMA associated with significant warming of tropopause as well as above and below the tropopause region in 2015.**

**However, to avoid confusion, we have removed that sentence from the abstract in the revised manuscript.**

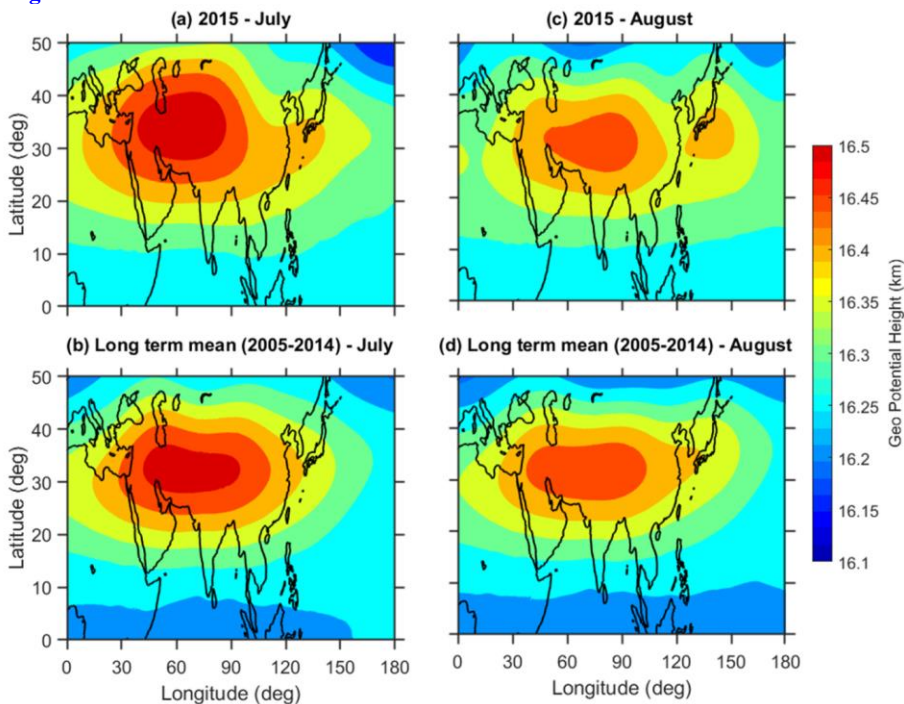
Page7Line152: About the methodology, the authors selected the long-term mean during the period of 2005-2014, why not include the data in 2015 when calculating the long-term mean? Please clarity.

**Reply: If we include the disturbed year also while calculating the climatology, it may bias the background. To see the exact variability of different trace gases and ASMA structure in 2015, we have not included the data of 2015 in long term mean.**

Page9: For Fig.2, do the authors check the distribution of the GPH using the ERA5 reanalysis data? Based on the results in Nützel et al., 2016, their research shows that only the NCEP reanalysis

311 data show a clear bimodal structure of the ASMA centers compared to other reanalysis data.  
312 Curious about the distribution of the GPH from the ERA-Interim/ERA5 data in 2015 and the long-  
313 term mean. Additionally, why not calculate the cold point tropopause and the temperature lapse  
314 rate tropopause using the same reanalysis data instead of the COSMIC data?

315 **Reply: As for reviewer suggestion, we have tried GPH spatial distribution in 2015 as well as**  
316 **long term mean (2005-2014 mean) by using ERA-5 reanalysis data. The observed GPH**  
317 **distribution was shown in below figure (Note that this figure was not included in the**  
318 **manuscript). We found a clear difference between NCEP reanalysis 2 and ERA 5 GPH in**  
319 **terms of GPH values. But both data show similar spatial structure of ASMA in 2015 as well**  
320 **long term mean.**



321  
322  
323 **Regarding tropopause from ERA-5: It is well established that the COSMIC RO is providing**  
324 **high accuracy and high vertical resolution temperature data particularly within the UTLS**  
325 **region. Several studies already have well reported about its usefulness towards tropopause**  
326 **structure and its variability. For this reason, we extensively utilized COSMIC RO data in**  
327 **our study.**

328 Page15: Fig.6 Black arrows can not be seen.

329 **Reply: Apologies for the mistake. We have included the arrows in the revised manuscript.**

330  
331  
332 Page22L393: This sentence should be rewritten. The tropopause within the ASMA is higher than

333 the outside regions at the same latitude.

334 **Reply: Corrected in the revised manuscript as suggested.**

335  
336 Page26Line477-480: ...enhanced ozone ...warms around the tropopause region and caused an  
337 increase in the UTLS temperature within the ASMA...leads to the weakening of the ASMA in  
338 2015. The statement is not clear. The authors mean enhanced ozone warms the tropopause within  
339 the ASMA ..and ..leads to the weakening of the ASMA in 2015. If it is true, the results from Figure  
340 3 show that the spatial extension of the ASMA is larger than the long-term mean in all the regions  
341 except over northeastern Asia in July 2015 as you mentioned in this manuscript. The authors did  
342 not present the connection between the large spatial extension of the Asian summer monsoon  
343 anticyclone and the weak monsoon. Enhanced O3 (decrease WV, CO), and positive tropopause  
344 temperature anomalies can be seen in July 2015 from your presents, but how the enhanced ozone  
345 leads to the weakening of the ASMA in July 2015 can not be seen in the paper.

346 **Reply: The changes in the O3 concentrations (increase/decrease) within the ASMA are one**  
347 **of the possible mechanisms to strengthening/weakening of the ASMA (Braesicke et al., 2011).**  
348 **By using idealized climate model experiments, Braesicke et al. (2011) clearly demonstrated**  
349 **that the strengthening (weakening) of the ASMA occurred when the O3 is decreased**  
350 **(increased) within the ASMA. The increased O3 within the ASMA warms the entire**  
351 **anticyclone region and weakens the ASMA (Braesicke et al., 2011). Our results from the**  
352 **present study are also in agreement with the results of Braesicke et al. (2011). We also**  
353 **observed a pronounced increase of O3 within the ASMA associated with significant warming**  
354 **of tropopause as well as above and below the tropopause region in 2015.**

355 **However, to avoid confusion, we have changed the sentence in the revised manuscript.**

356  
357 Citation corrections: Page12Line44: The reference Hossaini et al., 2015 is missing.

358 Randerl et al., 2010!Randel et al., 2010!ij§ Rightij§

359 **Reply: We have corrected and included the missed references in the revised manuscript.**

360  
361 Page13Line50: ... be found in Santee et al (2017)!... be found in Santee et al. (2017)

362 **Reply: Corrected as suggested.**

363  
364 Page22L389, L396: Ratnam et al., 2016 is missing, or is it Venkat Ratnam et al., 2016?

365 **Reply: Yes. It is Vekat Ratnam et al., 2016. We have modified as Venkat Ratnam et al., 2016**  
366 **in the revised manuscript.**

367  
368 Page30Line603: Li J. et al., 2008 and Li and Bian 2015 are missing in the main text. ...

369 **Reply: We have removed these references from the list in the revised manuscript.**

370  
371 The citation and references need to be edited thoroughly.

372 **Reply: Thanks for the suggestion. We have taken care about this in the revised manuscript**  
373 **as suggested by the reviewer.**

374  
375 Page9Line188: Fig. 2a and 2b (Fig. 2c and 2d)!Figs. 2a and 2b (Fig. 2c and 2d)

376 **Reply: Corrected in the revised manuscript.**

377  
378 Page14 Line266: 10-6 kg- im2s-2K, correct it.

379 **Reply: Corrected in the revised manuscript.**

380

381 Page14 Line274-275: Even!even, 04August ! 4August

382 **Reply: Corrected in the revised manuscript.**

383

384 Page17 Line314: Fig. 7a-c (Fig. 7d-f) show !Fig. 7a-c (Fig. 7d-f) shows

385 **Reply: Corrected in the revised manuscript.**

386

387 Page22 Line404: Fig. 10a-b (Fig. 10c-d) show!Fig. 10a-b (Fig. 10c-d) shows

388 **Reply: Corrected in the revised manuscript.**

389

390 Page25 Line447: Fig. 3 and 4!Figs. 3 and 4 ...

391 **Reply: Corrected in the revised manuscript.**

392

393 Suggest that the authors should read their final manuscript carefully, or find a proofreader before  
394 the paper was submitted.

395 **Reply: Thanks for the suggestion. In the revised version of the manuscript, we have taken  
396 utmost care to reduce the typos and grammatical mistakes to the maximum possible extent.**

397

398

399 **We once again thank the reviewers for going through the manuscript carefully and offering  
400 potential solutions which made us to improve the manuscript content further.**

401

—END—

402

403

404

405

406

Formatted: Font: Not Bold

407 **Structure, dynamics, and trace gases variability within the Asian**  
408 **summer monsoon anticyclone in extreme El Niño of 2015-16**

409 Saginela Ravindra Babu<sup>1,2\*</sup>, Madineni Venkat Ratnam<sup>2</sup>, Ghouse Basha<sup>2</sup>, Shantanu Kumar Pani<sup>1</sup>  
410 and Neng-Huei Lin<sup>1,3\*</sup>

411 <sup>1</sup>Department of Atmospheric Sciences, National Central University, Taoyuan 32001, Taiwan

412 <sup>2</sup>National Atmospheric Research Laboratory, Gadanki 517112, India.

413 <sup>3</sup>Center for Environmental Monitoring and Technology, National Central University, Taoyuan  
414 32001, Taiwan

415 \*Correspondence to: S.R.Ravindra Babu ([baburavindra595@gmail.com](mailto:baburavindra595@gmail.com)) and N.-H. Lin  
416 ([nhlin@cc.ncu.edu.tw](mailto:nhlin@cc.ncu.edu.tw))

Formatted: Left

417 **Abstract:** A weak El Niño during 2014-15 boreal winter was developed as a strong boreal summer  
418 event in 2015 which continued and even enhanced during the following winter. In this work, the  
419 detailed changes in the structure, dynamics and trace gases within the Asian summer monsoon  
420 anticyclone (ASMA) during extreme El Niño of 2015-16 is delineated by using Aura Microwave  
421 Limb Sounder (MLS) measurements, COSMIC Radio Occultation (RO) temperature, and NCEP  
422 reanalysis products. Our analysis concentrates only on the summer months of July and August  
423 2015 when Nino 3.4 index started to exceed 1.5 values. We have considered the individual months  
424 of July and August 2015 for the present study. The results show that the ASMA structure was quite  
425 different in summer 2015 as compared to the long-term (2005-2014) mean. In July, the spatial  
426 extension of the ASMA shows larger than the long-term mean in all the regions except over  
427 northeastern Asia, where, it exhibits a strong southward shift in its position. The ASMA splits into  
428 two and western Pacific mode is evident in August. Interestingly, the subtropical westerly jet (STJ)  
429 shifted southward from its normal position over northeastern Asia as resulted mid-latitude  
430 air moved southward in 2015. Intense Rossby wave breaking events along with STJ are  
431 also found in July 2015. Due to these dynamical changes in the ASMA, pronounced changes in

432 the ASMA tracers are noticed in 2015 compared to the long-term mean. A 30% (20%) decrease in  
433 carbon monoxide (water vapor) at 100 hPa is observed in July over most of the ASMA region,  
434 whereas in August the drop is strongly concentrated in the edges of the ASMA. Prominent increase  
435 of O<sub>3</sub> (>40%) at 100 hPa is clearly evident within the ASMA in July, whereas in August the  
436 increase is strongly located (even at 121 hPa) over the western edges of the ASMA. Further, the  
437 temperature around the tropopause shows significant positive anomalies (~5K) within the ASMA  
438 in 2015. ~~The present results clearly reveal the El Niño induced dynamical changes caused~~  
439 ~~significant changes in the trace gases within the ASMA in summer 2015. Overall, warming of the~~  
440 ~~tropopause region due to the increased O<sub>3</sub> weakens the anticyclone and further supported the~~  
441 ~~weaker ASMA in 2015 reported by previous studies.~~

442 **Keywords:** Trace gases, El Niño, Asian summer monsoon anticyclone, tropopause

## 443 1. Introduction

444 The Asian summer monsoon anticyclone (ASMA) is a distinct circulation system in the upper  
445 troposphere and lower stratosphere (UTLS) during northern hemisphere boreal summer, ~~and~~  
446 centered at ~25°N and ~~extends-extending~~ roughly between 15°N to 40°N (Park et al., 2004; Randel  
447 et al., 2010). It is encircled by the subtropical westerly jet stream to the north and by the equatorial  
448 easterly jet to the south (Randel and Park, 2006). It is well recognized that the ASMA circulation  
449 is a prominent transport pathway for troposphere pollutants to enter the stratosphere (Randel et al.,  
450 2010). Previous studies have concluded that deep convection during summer monsoon can  
451 effectively transport the pollutants, aerosols and tropospheric tracers from the boundary layer into  
452 the UTLS region (Vogel et al., ~~2015~~2016; Santee et al., 2017). These transported pollutants, tracers  
453 and aerosols become confined in the ASMA and, consequently, affect the trace gas composition in  
454 the UTLS region (Randerl et al., 2010; Solomon et al., 2010; Riese et al., 2012; Hossaini et al.,

455 2015). It is clearly evident from the previous studies that the ASMA has a higher concentrations  
456 of tropospheric tracers such as carbon monoxide (CO), hydrogen cyanide (HCN) and Methane  
457 (CH<sub>4</sub>) and lower concentrations of stratospheric tracers including Ozone (O<sub>3</sub>) and nitric acid  
458 (HNO<sub>3</sub>) (Park et al., 2004; Li et al., 2005; Park et al., 2008; Randel et al., 2010; Vernier et al.,  
459 2015; Yan and Bian, 2015; Yu et al., 2017; Santee et al., 2017; [Vernier et al., 2018](#)). The  
460 comprehensive study on the climatological composition ~~within~~ the ASMA can be found in  
461 Santee et al. (2017). The ASM convection and orographic lifting are the primary mechanisms for  
462 the higher concentrations of the tropospheric tracers in the ASMA (Li et al., 2005; Park et al.,  
463 ~~2007~~[2009](#); Santee et al., 2017). Apart from these trace gases a strong persistent tropopause-level  
464 aerosol layer called as ‘Asian Tropopause Aerosol Layer’ (ATAL) also existed between 12 to 18  
465 km within the ASMA and it was first detected from the CALIPSO measurements (Vernier et al.,  
466 2011).

467 Similarly, higher concentrations of water vapor (WV) within the ASMA during the summer  
468 monsoon is well documented in the literature (Gettelman et al., 2004; Park et al., 2007; Randel et  
469 al., 2010; Bian et al., 2012; Xu et al., 2014; Jiang et al., 2015; Das and Suneeth, 2020). ~~It is~~ ~~W~~well  
470 known that ~~the~~ most of the ~~water vapor~~ ~~WV~~ enters the stratosphere through the tropical tropopause  
471 ~~layer~~ (Fueglistaler et al., 2009) and the temperature ~~presented~~ at the tropical tropopause ~~strongly~~  
472 controls the WV entering the lower stratosphere (LS). It is ~~also~~ well documented that several  
473 processes such as convection, strength of the Brewer-Dobson circulation, El Niño–Southern  
474 Oscillation (ENSO) and Quasi-Biennial Oscillation (QBO) are responsible for the WV transport  
475 to the UTLS region (Holton et al., 1995; ~~Jiang et al., 2010~~; Dessler et al., 2014; Jiang et al., 2015;  
476 ~~Das and Suneeth, 2020~~). ~~Other factors such as gravity waves and horizontal advection can also~~  
477 ~~influence the WV transport in the UTLS region. For example,~~ Khan and Jin (2016), studied the

478 effect of gravity waves on the tropopause and WV ~~in the over~~ Tibetan Plateau and reported that the  
479 gravity wave is the source for the WV transport from the lower to higher altitudes. ~~The tropopause~~  
480 ~~is higher within the ASMA during the summer monsoon period as compared the surrounding~~  
481 ~~regions (Randel et al., 2010; Santee et al., 2017).~~ Recently, Das and Suneeth (2020) reported about  
482 the distributions of WV in the UTLS over the ASMA during summer using 13 years of Aura  
483 Microwave Limb Sounder observations. They concluded that WV in the UTLS region inside the  
484 central part of ASMA is mostly controlled by horizontal advection and very less from the local  
485 process and tropopause temperature in both summer and winter. ~~reported about the causative~~  
486 ~~mechanism for the presence of high WV in the ASMA region. The authors concluded that the~~  
487 ~~UTLS water vapor in the ASMA is mainly controlled by the advection and tropopause altitude.~~

488 Convection during the summer monsoon is one of the major sources to transport the boundary  
489 layer pollutants into the UTLS region (Randel et al., 2010). It is well established fact that the ENSO  
490 has a strong influence on convection and circulation changes over the Asian monsoon region  
491 (Kumar et al., 1999; Wang et al., 2015; Gadgil and Francis, 2016). Enhanced (suppressed)  
492 convection over the Asian monsoon region generally observed in the cold phase of ENSO (warm  
493 phase of ENSO) known as La Niña (El Niño). Few studies have existed to date on the impact of  
494 ENSO on the ASMA trace gas composition changes and its dynamical changes. For example, Yan  
495 et al. (2018) reported the influence of ENSO on the ASMA with a major focus on how the ENSO  
496 winter signal propagates into the following seasons. They showed the weaker O<sub>3</sub> transport into the  
497 tropics during the onset of the ASMA after boreal winter El Niño events, but the difference between  
498 El Niño and La Niña composites becomes insignificant in the summer. In another study, Tweedy  
499 et al. (2018) demonstrated the impact of boreal summer ENSO events on O<sub>3</sub> composition within  
500 the ASMA in different phases of ENSO events. They reported that the ASMA forms earlier and

501 stronger in the La Niña period that leads to greater equatorward transport of O<sub>3</sub>-rich air from the  
502 extra-tropics into the northern tropics than during El Niño periods. ~~Very +R~~Recently, Fadnavis et al.  
503 (2019) reported higher concentrations of aerosol layers observed in the ATAL region during the El  
504 Niño period over the northern part of South Asia. However, the above- mentioned studies are  
505 mainly focused on changes in the ASMA with respect to ENSO on seasonal scales or mature stage  
506 of monsoon (combined mean of July and August), ~~respectively~~.

507 Based on the above-mentioned studies, it ~~is can be~~ concluded that the ENSO also has a strong  
508 influence on the ASMA structure and its composition. The recent 2015-16 El Niño event was  
509 recorded as an extreme and long-lasting event in the 21<sup>st</sup> century (Huang et al., 2016; Avery et al.,  
510 2017). It was started as a weak El Niño during 2014-15 boreal winter and it developed as a strong  
511 boreal summer El Niño event in 2015 (Tweedy et al., 2018). Further, this strong boreal summer  
512 event was continued and significantly enhanced until the boreal winter of 2015-16. It was also one  
513 of the strongest El Niño events that occurred in the boreal summer (Tweedy et al., 2018). In this  
514 event, several unusual changes occurred in the tropical UTLS region including, the strong  
515 enhancement in the lower stratosphere WV (higher positive tropopause temperature anomalies)  
516 over ~~the~~ Southeast Asia and western Pacific regions (Avery et al., 2017) and anomalous distribution  
517 of trace gases in the UTLS region (Diallo et al., 2018; Ravindra Babu et al., 2019a). Similar way,  
518 the response of different trace gases (O<sub>3</sub>, HCl, WV) to the disrupted 2015–2016 quasi-biennial  
519 oscillation (QBO) associated with 2015-16 El Niño event is also reported by Tweedy et al. (2017).  
520 Dunkerton (2016), discussed the possible role of unusual warm ENSO event in 2015-2016 to the  
521 QBO disruption by triggering the extratropical planetary waves. Therefore, in the present study,  
522 we ~~tried to investigate~~ the detailed changes observed in the ASMA 2015 particularly by focused  
523 focusing on the structure, dynamics and trace gases variability within the ASMA in July and

Formatted: Subscript

524 August 2015 by using satellite ~~measurements-observations~~ and reanalysis products. The present  
525 research article is organized as follows. A ~~d~~Database and methodology adopted in this study are  
526 discussed in Section 2. The results and discussions are illustrated in Section 3. Finally, the  
527 summary and conclusions obtained from the present study are summarized in Section 4.

## 528 **2. Database and Methodology**

### 529 **2.1. Microwave Limb Sounder (MLS) measurements**

530 In the present study, version 4.2 Aura MLS measurements of CO, O<sub>3</sub> and WV are utilized.  
531 The MLS data of July and August months in each year from 2005 to 2015 period are considered.  
532 The vertical resolution for CO is in the range 3.5–5 km from the upper troposphere to the lower  
533 mesosphere and the useful range is 215–0.0046 hPa. The horizontal resolution for CO is about 460  
534 km at 100 hPa and 690 km at 215 hPa. For WV, the vertical resolution is in the range of 2.0 to 3.7  
535 km from 316 to 0.22 hPa and the along-track horizontal resolution varies from 210 to 360 km for  
536 pressure greater than 4.6 hPa. For O<sub>3</sub>, the vertical resolution is ~2.5 km and the along-track  
537 horizontal resolution varies between 300 and 450 km. The precision (systematic uncertainty) for  
538 WV is ~ 10-40% (~10-25%), for O<sub>3</sub> is ~0.02–0.04 (~0.02–0.05) ppmv and for CO, it is ~ 19 ppbv  
539 (30%), respectively. More details about the MLS version 4 level 2 data can be found in Livesey et  
540 al. (2018).

### 541 **2.2. COSMIC Radio Occultation measurements**

542 To see the changes in the tropopause temperature and height within the ASMA, we used high-  
543 resolution, post-processed products of level 2 dry temperature profiles obtained from Constellation  
544 Observing System for Meteorology, Ionosphere, and Climate (COSMIC) Radio Occultation (RO).  
545 Each month of July and August from 2006 to 2015 are considered. The data is downloaded from  
546 the COSMIC Data Analysis and Archival Center (CDAAC) website. We used 200 m vertical

547 resolution temperature profiles in the study. Details of the temperature retrieval from the bending  
548 angle and refractivity profiles obtained from the RO sounding are presented well in the literature  
549 (Kursinski et al. 1997; Anthes et al. 2008). The COSMIC temperature have a precision of 0.1%  
550 between 8 and 25 km (Kishore et al. 2009; Kim and Son, 2012). The temperature accuracy in the  
551 UTLS is better than 0.5 K for individual profiles and ~0.1 K for averaged profiles (Hajj et al.  
552 2004). It is noted that for individual RO temperature profiles, the observational uncertainty  
553 estimate is 0.7 K in the tropopause region, slightly decreasing into the troposphere and gradually  
554 increasing into the stratosphere (Scherllin-Pirscher et al., 2011a). For monthly zonal-averaged  
555 temperature fields, the total uncertainty estimate is smaller than 0.15 K in the UTLS (Scherllin-  
556 Pirscher et al., 2011b). Overall, the uncertainties of RO climatological fields are small compared  
557 to any other UTLS observing system for thermodynamic atmospheric variables. Note that these  
558 data are compared with a variety of techniques including GPS radiosonde data and observed good  
559 correlation particularly in the UTLS region (Rao et al. 2009; Kishore et al. 2009). The COSMIC  
560 RO profiles have been widely used for studying the tropopause changes and its variabilities (Kim  
561 and Son, 2012; RavindraBabu et al. 2015; [RavindraBabu and Liou, 2021](#)).~~RavindraBabu et al.~~  
562 ~~2019b~~).

### 563 **2.3. National Centers for Environmental Prediction (NCEP) Reanalysis data**

564 We also utilized monthly mean Geopotential height (GPH) and wind vectors (zonal and  
565 meridional wind speed) from the [NCEP-DOE Reanalysis 2 \(Kanamitsu et al., 2002\)](#),~~National~~  
566 ~~Centers for Environmental Prediction/National Center for Atmospheric Research (NCEP/NCAR)~~  
567 ~~reanalysis (Kalnay et al., 1996)~~, covering the same time period as the MLS observations (2005-  
568 2015). [NCEP-DOE Reanalysis 2 is an improved version of the NCEP Reanalysis I model that](#)  
569 [fixed errors and updated parametrizations of physical processes.](#) The horizontal resolution of

570 ~~NCEP/NCAR~~ NCEP-DOE Reanalysis 2 is  $2.5^\circ \times 2.5^\circ$ , respectively.

571 Apart from the above-mentioned data sets, we also used European Centre for Medium-Range  
572 Weather Forecasts (ECMWF) interim reanalysis potential vorticity (PV) data particularly at 350K  
573 isentropic surface in July and August 2015 (ERA-Interim; Uppala et al., 2005; Dee et al., 2011).

### 574 **2.5. Methodology**

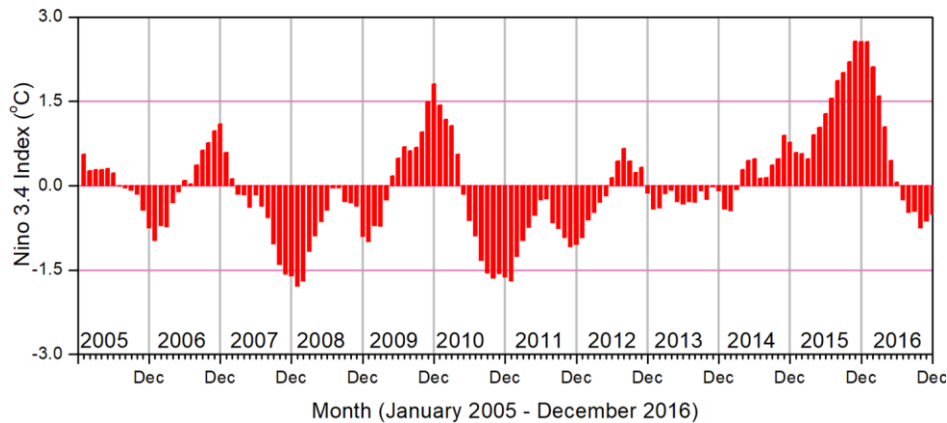
575 Daily available MLS profiles of O<sub>3</sub>, CO, and WV in each month are constructed and gridded  
576 by averaging the profiles inside bins with a resolution of  $5^\circ$  latitude  $\times$   $5^\circ$  longitudes. The following  
577 equation is used to estimate the relative change in percentage.

$$578 \text{ Relative change in percentage} = \left( \frac{x_i - \bar{x}}{\bar{x}} \right) \times 100 \quad (1)$$

579 where  $x_i$  represents the monthly mean of July/August in 2015, and  $\bar{x}$  is the corresponding monthly  
580 long-term mean which is calculated by using the data from 2005 to 2014.

### 581 **3. Results and Discussion**

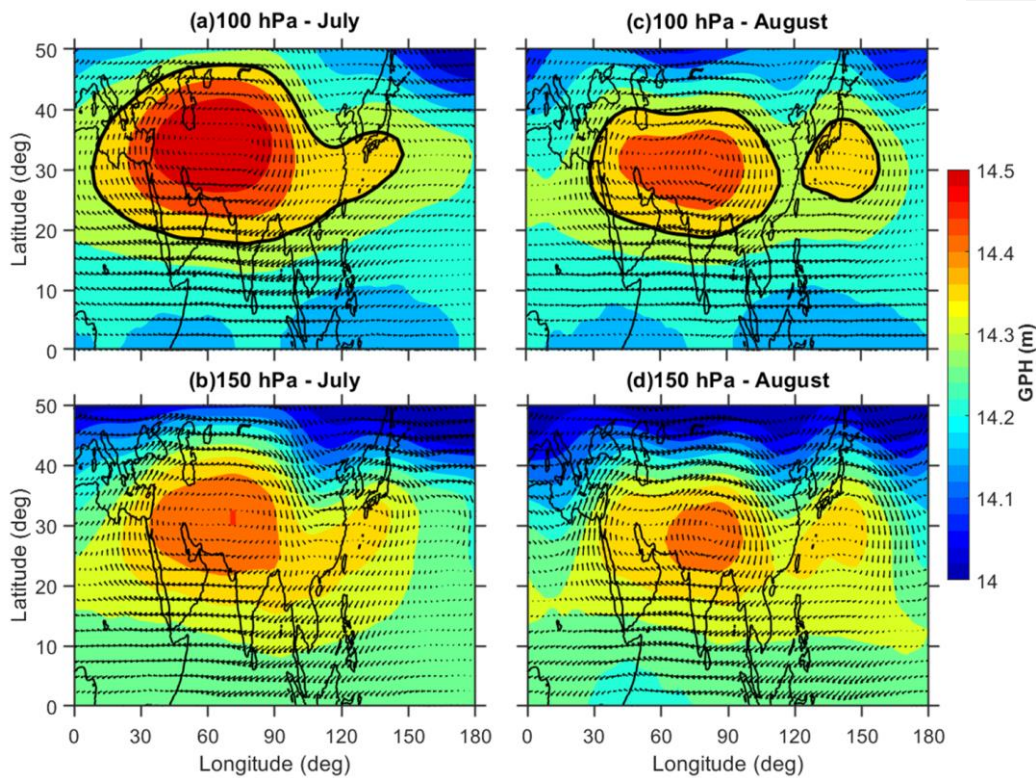
582 It is well reported that the ASMA is highly dynamic in nature with respect to its position and shape.  
583 Also it varies at different time scales i.e day-to-day, weekly and monthly scales caused by internal  
584 dynamical variability (Randel and Park, 2006; Garny and Randel, 2013; Pan et al., 2016; Nützel  
585 et al., 2016; Santee et al., 2017). The intensity and spatial extension of the ASMA are prominent  
586 in July and August where the monsoon was in the mature phase (Santee et al., 2017; Basha et al.,  
587 2019). It can be noticed that the 2015-16 El Niño event was one of the strongest boreal summer  
588 events that occurred in the entire MLS data record (Tweedy et al., 2018). In this event, the Nino  
589 3.4 data was exceeded +1.5 in July and +1.8 in August (**Fig. 1**). Therefore, in the present study,  
590 we mainly focused on ASMA behavior and trace gases changes ~~in~~ within the ASMA on monthly  
591 scales particularly in July and August 2015 which represents strong El Niño.



592  
 593 **Figure 1.** Temporal evolution of observed Niño3.4 Index data from January 2005 to December  
 594 2016.

595 **3.1. Structure and dynamical changes in ASMA during 2015**

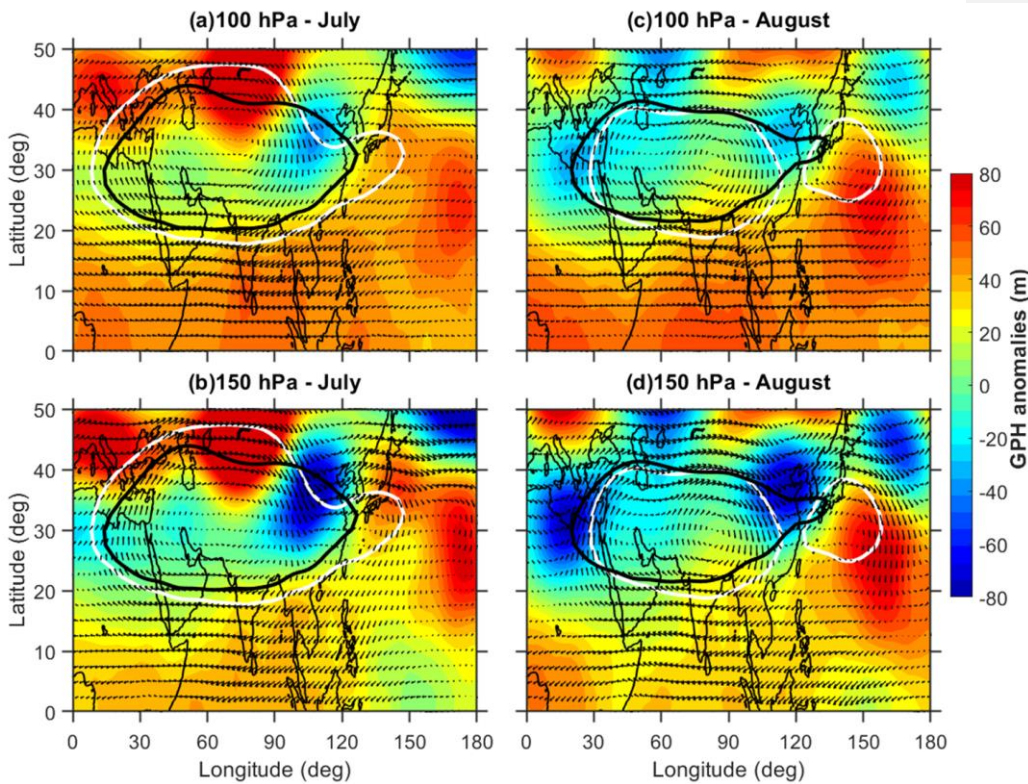
596 In general, the studies looking at monthly or seasonal timescales related to the thermo-  
 597 dynamical features in the ASMA, the anticyclone region is mostly defined from the simple  
 598 constant GPH contours at different pressure levels (Randel and Park, 2006; Yan et al., 2011;  
 599 Bergman et al., 2013; Basha et al., 2019). Previous researchers used different GPH contours at 100  
 600 hPa to define the anticyclone region. For example, Yan et al. (2011) used 16.7 km, Bergman et al.  
 601 (2013) used 16.77 km and recently Basha et al. (2019) used 16.75 km GPH contour as the  
 602 anticyclone region. In a similar manner, we also defined the ASMA region based on [NCEP-DOE](#)  
 603 [Reanalysis 2 obtained NCEP reanalysis](#) GPH at 100 hPa and considered the 16.75 km GPH contour  
 604 as the anticyclone region.



605  
 606 **Figure 2.** Spatial distribution of geopotential height ~~observed~~ obtained from NCEP-DOE  
 607 Reanalysis 2 data in during July 2015 (a) at 100 hPa and (b) 150 hPa superimposed with wind  
 608 vectors at the respective corresponding levels. Subplots of (c) and (d) are the same as (a) and (b)  
 609 but for the month of August. The black color solid contour lines represent the ASMA region at 100  
 610 hPa (16.75 km GPH contour).

611 The spatial distribution of GPH at 100 hPa and 150 hPa for the month of July (August) is  
 612 shown in **Fig. 2a and 2b (Fig. 2c and 2d)**. The corresponding monthly mean winds at respective  
 613 pressure levels are also shown in **Fig.2**, respectively. The black solid line represents the ASMA  
 614 region at 100 hPa based on 16.75 km GPH contour. The GPH distribution in **Fig. 2** shows clear  
 615 distinct variability in the ASMA spatial structure between July and August at both pressure levels.

616 For example, at 100 hPa, the maximum GPH center was located over western side in July whereas  
617 it was located over near to the Tibetan region in August. Interestingly the ASMA itself separated  
618 into two anticyclones (16.75 km GPH contour black solid line in the figure) in August compare to  
619 July. The center of the small anticyclone was located over the ~~northwestern~~Northwestern pacific  
620 Pacific near 140°E with the closed circulation indicated by the wind arrows.  
621



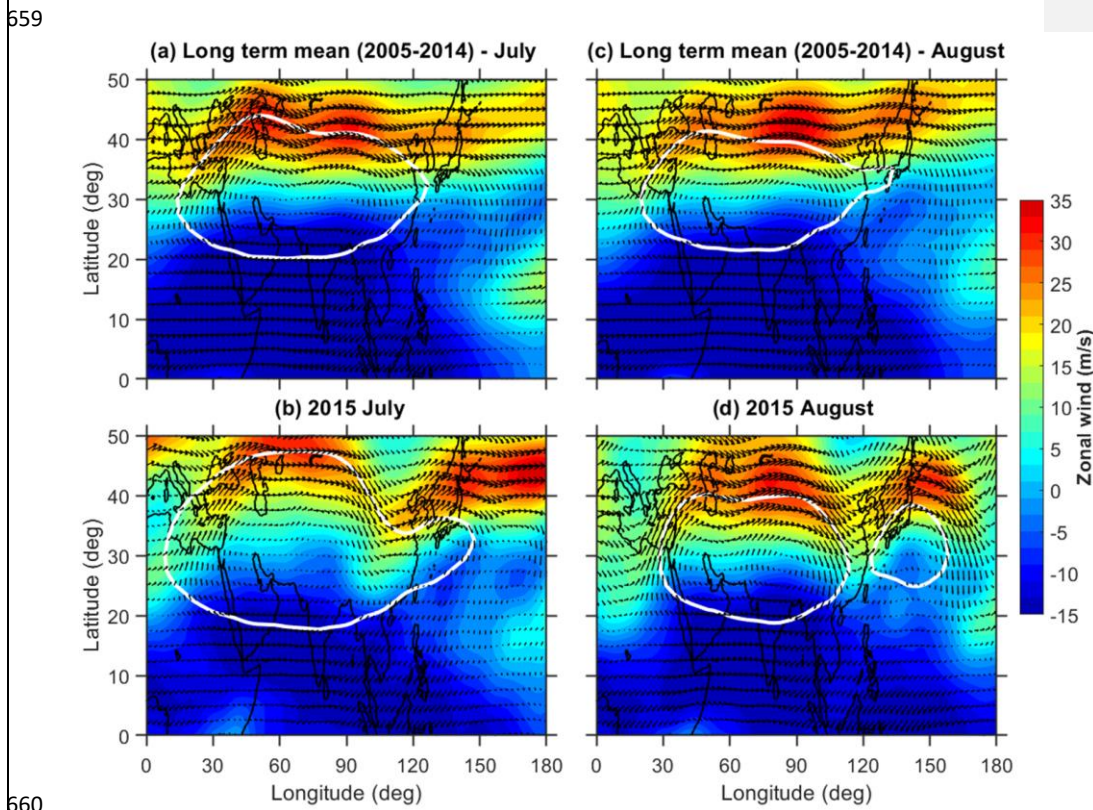
622  
623 **Figure 3.** Spatial distribution of geopotential height anomalies obtained from NCEP-DOE  
624 Reanalysis 2 data ~~observed in~~ observed in during July 2015 (a) at 100 hPa and (b) 150 hPa superimposed with  
625 wind vectors at the respective corresponding levels. (c) and (d) same as (a) and (b) but for the  
626 month of August. The white color solid contour lines represent the ASMA region at 100 hPa (16.75

627 km GPH contour) observed in 2015 whereas the black color line represents the mean of 2005-  
628 2014.

629 Further, we compared the ASMA structure in 2015 with referenced long-term mean. For  
630 this, we obtained the GPH anomalies by subtracting the background long-term mean (2005-2014)  
631 from 2015. **Fig-3Figure 3** shows the latitude-longitudinal distribution of GPH anomalies (color  
632 shaded) along with wind vectors depicting circulation pattern at 100 hPa as well as at 150 hPa  
633 during July and August. The white (black) color contour represents 16.75 km GPH at 100 hPa for  
634 the corresponding month in 2015 (long-term mean). The GPH anomalies at both pressure levels  
635 show quite different features in July and August. A clear wave-like structures can be observed  
636 from the GPH anomalies. In July, the GPH anomalies exhibit strong negative maxima over 25-  
637 40°N, 90-120°E and positive maxima over 40-50°N, 60-80°E regions. The 16.75 km GPH contour  
638 lines in the ASMA region exhibits higher extension in all the directions except over the  
639 northeastern edges of the ASMA in July compared to the long-term mean. At the same location  
640 (northeastern edges), the ASMA exhibits a pronounced southward extension in July. Distinct  
641 features of GPH anomalies are noticed in August as compared to July. In August, the strong  
642 negative GPH anomalies are situated over the west and north-eastern edges of the ASMA.

643 It is well known that the subtropical westerly jet is an important characteristic feature of  
644 the ASMA (Ramaswamy 1958), and thus its changes during 2015 are also investigated. As the  
645 peak intensity of the westerly jet was located at 200 hPa (Chiang et al., 2015), we focused mainly  
646 on 200 hPa zonal wind changes in July and August. **Fig-Figure 4a and 4c (Fig. 4b and 4d)** show  
647 the spatial distribution of long-term (2015) monthly mean zonal wind at 200 hPa during July and  
648 August. In general, the subtropical westerlies are located near to ~40°N latitude during the mature  
649 phase of the monsoon period (Chiang et al., 2015). Compared to long-term mean, a significant  
650 weakening of the subtropical westerlies is noticed in 2015. Further, a strong southward shift in the

651 westerlies is observed over the northeastern Asia region. This southward shift is moved even up  
652 to 30°N in both months. From zonal wind at 200 hPa (**Fig. 4**) and wind vectors at 100/150 hPa  
653 (**Fig. 2**), it is clear that anomalous changes have occurred in the subtropical westerlies over the  
654 northeastern parts of the AMSA around 30-40°N, 90-120°E during July and August 2015. The  
655 southward shift in the westerlies is strongly associated with the southward extension of the ASMA  
656 over the northeastern side of the ASMA (**Fig. 2**). This is strongly supported by the previous  
657 findings by Lin and Lu (2005) where they showed the southward extension of the South Asian  
658 High could lead to the southward shift of the ~~westerly~~westerlies.



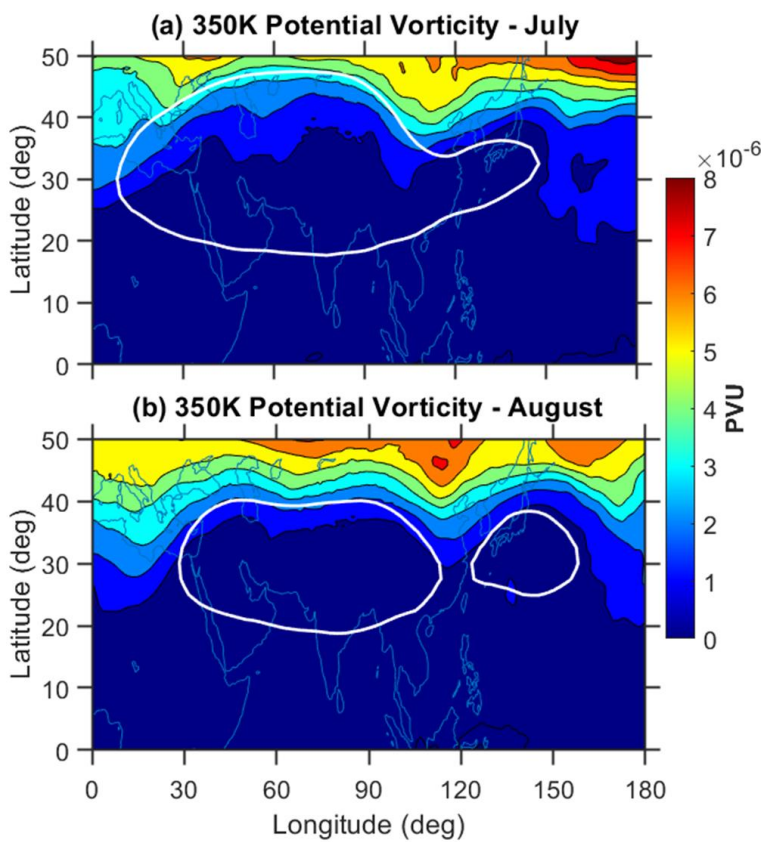
660 **Figure 4.** Spatial distribution of monthly mean zonal winds ~~observed~~obtained from NCEP-DOE  
661

662 Reanalysis 2 data at 200 hPa ~~in~~-during July during (a) 2005-2014 (b) 2015 year. (c) and (d) same  
663 as (a) and (b) but for the month of August. The white color solid contour lines represent the ASMA  
664 region at 100 hPa (16.75 km GPH contour).

665 From the GPH and winds observations, it is clear that pronounced changes are evident in  
666 the dynamical structure of the ASMA in 2015 and also relatively different features are noticed  
667 between July and August months. Interestingly the ASMA itself separated into two anticyclones  
668 during August 2015 and the separation exactly coincided with the strong negative GPH anomalies  
669 and southward meandering of subtropical westerlies over the northeastern side of the ASMA. The  
670 ~~western-Western pacific-Pacific (WP)~~ mode of the anticyclone is visible in August. The split of  
671 the anticyclone and the formation of the ~~western-Pacific (WP)~~ mode are in agreement with previous  
672 studies reported by few researchers earlier (e.g. Homomichl and Pan, 2020). The presence of the  
673 WP mode may be due to the eastward eddy shedding of the ASMA system in the process of its  
674 sub-seasonal zonal oscillation (Homomichl and Pan, 2020) or Rossby wave breaking (RWB) in the  
675 subtropical westerly jet (Fadnavis and Chattopadhyay, 2017). Fadnavis and Chattopadhyay (2017)  
676 also identified the split of ASMA into two anticyclones: one over Iran and another over the Tibetan  
677 region due to the RWB in June 2014 monsoon period. To see any signatures of these RWB in 2015,  
678 we further analyzed the RWB through the ERA interim reanalysis potential vorticity (PV) data.  
679 Based on previous studies, it is reported that RWBs can be identified from PV distribution at 350  
680 K isentropic surface (Samanta et al. 2016; Fadnavis and Chattopadhyay, 2017). We used 350\_K  
681 isentropic surface PV data in July and August 2015 in the present analysis.

682 **Figure 5a–b** shows the distribution of ERA interim monthly mean PV at the 350 K  
683 isentropic surface during July and August 2015. It can be seen that, during July and August 2015,  
684 clear RWB signatures evident near 100°E. It is noted that the equatorial advection of high PV  
685 values with a steep gradient and the southward movement of PV from the westerly jet are the basic

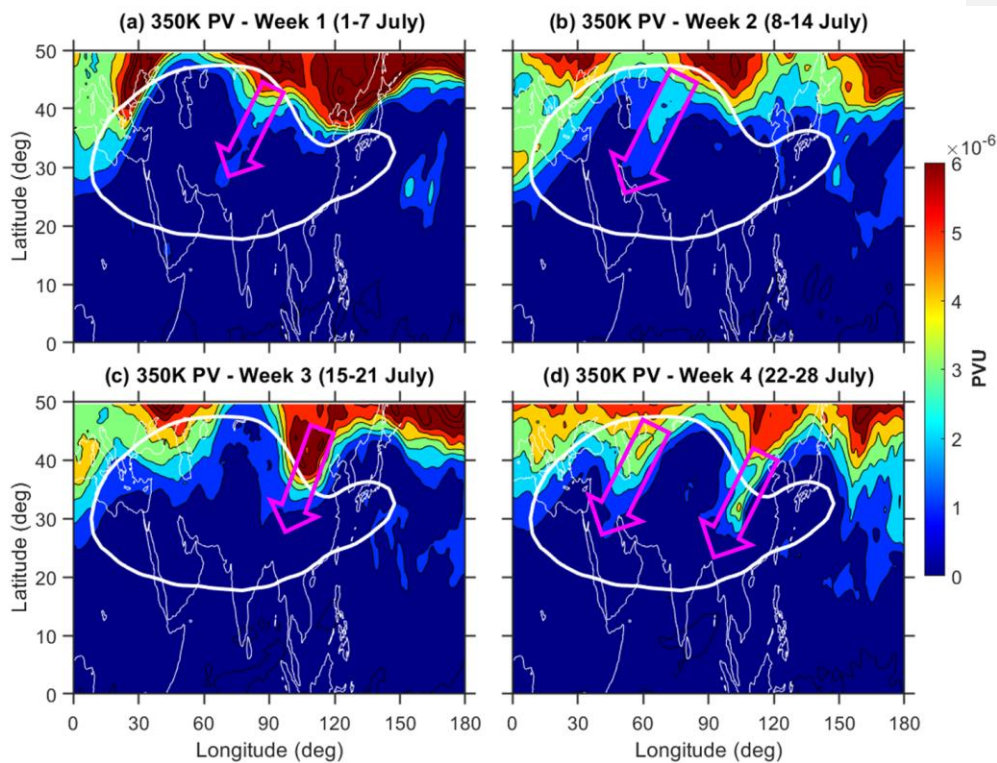
686 features of the RBW (Vellore et al., 2016; Samanta et al. 2016). These features are clearly exhibited  
687 in **Figure 5** with higher PV values extends up to  $\sim 30^\circ\text{N}$  in both months over  $100^\circ\text{E}$  region. The  
688 location of this RBW is significantly correlated with a southward meandering of westerlies and  
689 strong negative GPH anomalies. However, the observed RBW signatures in both months are from  
690 monthly mean PV data. Further, to see the clear signatures of these RBW, we made weekly based  
691 analysis for July month. For this we considered 1-7 July as week-1 and 8-14 July as week-2 so on.  
692 The weekly mean distribution of 350K isentropic surface PV during July is shown in **Figure-Fig.**  
693 **6**.



694

695 **Figure 5.** ERA Interim observed spatial distribution of potential vorticity (PV) on a 355-350 K  
696 isentropic surface in PVU ( $1 \text{ PVU} = 10^{-6} \text{ K m}^2 \text{ kg}^{-1} \text{ s}^{-1}$ ) ( $10^{-6} \text{ kg m}^2 \text{ s}^{-2} \text{ K}$ ): (a) monthly mean of  
697 July and (b) monthly mean of August 2015. The white color solid contour lines represent the  
698 ASMA region at 100 hPa (16.75 km GPH contour). Red color contours represent the anticyclone  
699 region during the respective months. The outer contour represents 16.75 km and the inner contour  
700 for 16.85 km geopotential height. Black arrows indicate the regions of RWB.  
701 The black-magenta colored arrows which are shown in the figure-Fig. 6 represents the RWB events  
702 during July 2015. A clear signature of air with high values of PV traverses from extra-tropics to  
703 ASMA is evident from Fig.6. At weekly scales, clear RWB signatures are observed over the  
704 anticyclone region. For example, in week-1 and week-2, the RWB signatures are evident over the  
705 northern region of the ASMA. However, in week-3 and week-4, these RWB signatures are very  
706 clear over northeastern Asia. Even-even in week-5 (29July-04August), we noticed RWB signatures  
707 in PV data (Figure not shown). This clearly shows that The RWB splits the ASMA into two  
708 anticyclones: one over the Tibetan region and another over the WP region. It is clear that the  
709 equatorward penetration of extra tropical forcing through the subtropical westerly jet is has started  
710 in July and further amplified by the splitting of the ASMA into two during August.

Formatted: Superscript



711  
 712 **Figure 6.** Same as **Figure 5**, but for the weekly distribution of PV in July 2015. **Black-Magenta**  
 713 **colored** arrows indicate the regions of RWB.

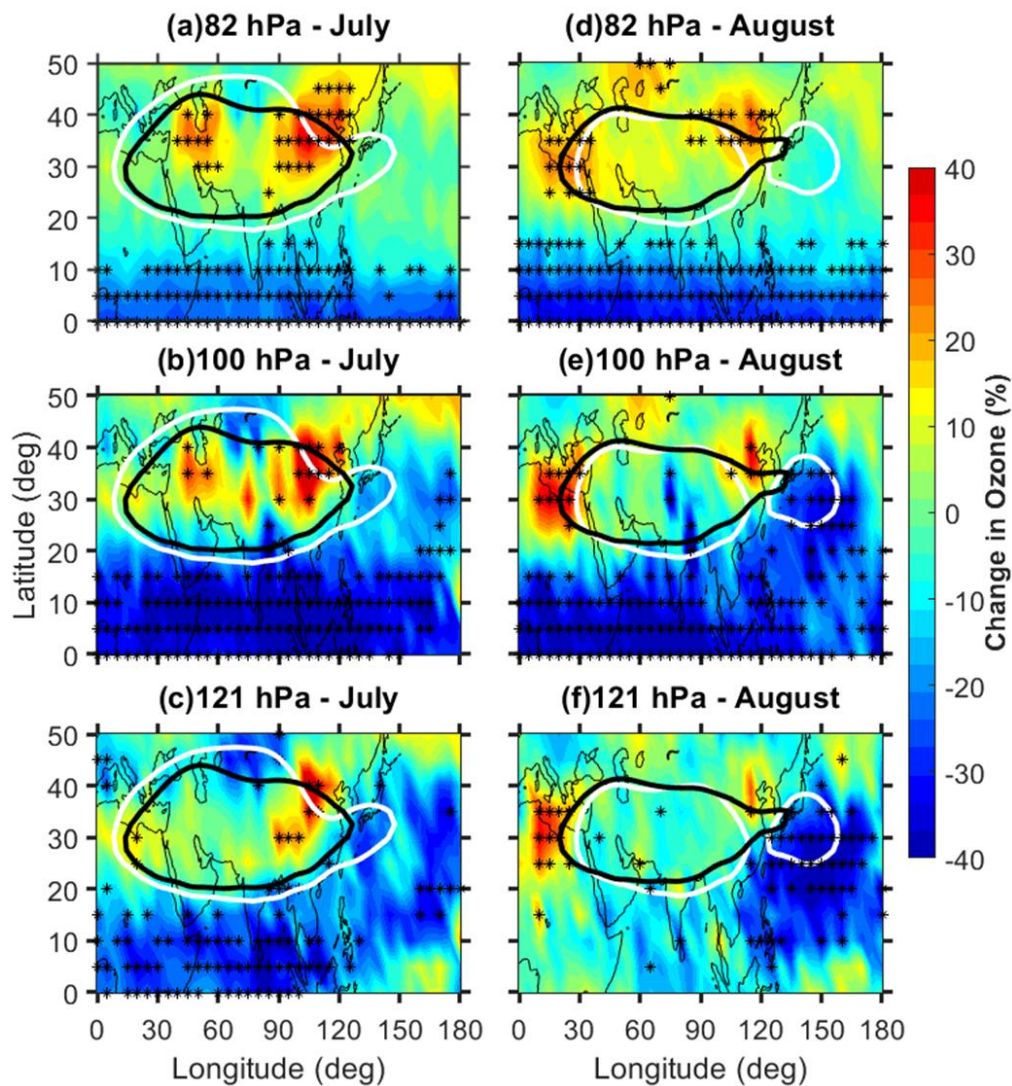
714 It is well known that the RWB is an important mechanism for horizontal transport between  
 715 the extratropical lower stratosphere to the tropical UTLS region. These RWBs can act as an agent  
 716 for the transport of extratropical stratospheric cold, dry, and O<sub>3</sub>-rich air into the ASMA during the  
 717 summer monsoon. Overall, it is concluded that the combination of the RWBs and strong southward  
 718 meandering of the subtropical westerly jet in 2015 causes significant dynamical and structural  
 719 changes in the ASMA. These changes in the ASMA dynamical structure in 2015 can influence the  
 720 concentrations of the different trace gases within the ASMA. **Further, we quantified the changes**  
 721 **in O<sub>3</sub>, CO and WV concentrations within the ASMA during 2015 caused by the dynamical**

Formatted: Subscript

722 ~~effects. Further we studied how much percentage change occurred in the O<sub>3</sub> concentration and other~~  
723 ~~tropospheric tracers with in the ASMA during 2015 due to these dynamical changes. For this we~~  
724 ~~extensively utilized MLS satellite trace gases measurements.~~ The changes that occurred in the O<sub>3</sub>  
725 and CO, WV, are discussed in the following sections.

### 726 3.2. Trace gases anomalies observed within the ASMA in 2015

727 ~~It is well-documented that the ASMA contains low (high)~~ Well reported that the ASMA has  
728 ~~low (high)~~ concentrations of stratospheric tracers such as O<sub>3</sub> (tropospheric tracers such as CO, WV  
729 and etc.) and higher tropopause height compared to the region outside the ASMA during boreal  
730 summer (Park et al., 2007; Randel et al., 2010; Santee et al., 2017; Basha et al., 2019). Differences  
731 ~~of the trace gases within and outside of the ASMA are attributed to~~ Remarkable variabilities of  
732 ~~these trace gases are attributed to~~ the strong winds and closed streamlines associated with the  
733 ASMA, which act to isolate the air (Randel and Park 2006; Park et al. 2007). ~~As mentioned in the~~  
734 ~~introduction, the monsoon in 2015 was strongly affected by the strong El Niño conditions in July~~  
735 ~~and August 2015. Based on the previous studies, the summer monsoon in 2015 was reported as a~~  
736 ~~weaker monsoon and the ASMA circulation also relatively weak (Yuan et al., 2018; Tweedy et al.,~~  
737 ~~2018).~~ To see the changes in the trace gases during 2015, we generated the background long-term  
738 mean of CO, O<sub>3</sub>, and WV by using 10 years of MLS trace gas data from 2005 to 2014. Here the  
739 results are discussed mainly based on the percentage changes relative to the respective long-term  
740 monthly mean trace gases using Equation Equ. 1.



742  
 743 **Figure 7.** Ozone relative percentage change in July 2015 with respect to background  
 744 climatological monthly mean observed at (a) 82 hPa, (b) 100 hPa and (c) 121 hPa. (c) and (d) same  
 745 as (a) and (b) but for the month of August. The white (black) color contour represents 16.75 km  
 746 geopotential height at 100 hPa for the corresponding month in 2015 (mean of 2005-  
 747 2014 climatological). The star symbols (black) shown in figure represent the anomalies greater than

748 the  $\pm 2\sigma$  standard deviation of long-term mean. The results are obtained from MLS measurements.  
749 **Fig-Figure 7a-c (Fig. 7d-f)** shows the distribution of relative percentage change in the O<sub>3</sub>  
750 concentrations within the ~~anticyclone~~ ASMA at 82 hPa, 100 hPa and 121 hPa during July (August)  
751 2015. The anomalies larger than  $\pm 2\sigma$  standard deviation of long-term mean are highlighted with  
752 star symbols in the respective figures. The spatial distribution of changes in the O<sub>3</sub> (Fig. 7) shows  
753 a clear increase in the O<sub>3</sub> mixing ratios (>40%) within the ASMA in 2015. The observed increase  
754 within the ASMA is quite distinct between July and August. In July, the O<sub>3</sub> shows a pronounced  
755 increase within the ASMA at all the pressure levels. Note that the observed increase was  
756 statistically significant with larger than  $2\sigma$  standard deviation of long-term mean (see the star  
757 symbols). This increase is quite significant over the northeastern edges of the ASMA and quite  
758 high at 100 hPa compared to 82 hPa and 121 hPa. In August, the O<sub>3</sub> shows quite different features  
759 compared to July (Fig. 7d-f). A strong increase in the O<sub>3</sub> is observed over the western and eastern  
760 edges of the ASMA at all the pressure levels. The increase is quite significant at 100 hPa and even  
761 at 121 hPa. The increase of O<sub>3</sub> is still appearing over the northeastern edges of the ASMA in August  
762 as observed in July. Overall, a significant enhancement of O<sub>3</sub> within the ASMA is clear evidence  
763 in July and August 2015.

764 The significant increase of O<sub>3</sub> within the ASMA in 2015 might be due to the transport from  
765 the mid-latitudes through the STJ and also due to the stratosphere to the troposphere transport. For  
766 example, the strong enhancement of O<sub>3</sub> within the ASMA at 100 hPa in July was strongly matched  
767 with the observed high values of PV at 350 K isentropic surface (Fig. 6). This is further supported  
768 by the strong southward meandering of STJ in July (Fig. 3), respectively. Thus, a clear transport  
769 of mid-latitude air with high PV and high O<sub>3</sub> is evident during 2015. At the same time, the  
770 enhancement of O<sub>3</sub> was clearly observed at all the pressure levels from 82 hPa to 121 hPa which  
771 is further supported for the stratosphere to the troposphere transport. Note that 82 hPa can represent

Formatted: Subscript

772 the lower stratosphere and 121 hPa for the upper troposphere (Das et al., 2020). It can be noticed  
773 that the ASMA is strongly associated with troposphere-stratosphere transport as well as  
774 stratosphere-troposphere transport (Garny and Randel, 2016; Fan et al., 2017). Also, it is well  
775 reported that the northern part of the ASMA is an active region for stratosphere-troposphere  
776 transport processes (Sprenger et al., 2003; Škerlak et al., 2014).

777 Similarly, significant lowering of O<sub>3</sub>, particularly at 100 hPa and 82 hPa is clearly noticed  
778 over the tropics (Fig. 7). This is quite expected due to the enhanced tropical upwelling (bringing  
779 poor O<sub>3</sub> air from troposphere) caused by the strong El Niño conditions in July and August 2015.

780 As mentioned in the previous sections, strong El Niño conditions are clearly evident in July and  
781 August 2015 (Fig. 1). The observed strong negative O<sub>3</sub> anomalies over the tropics from the present  
782 study are well matched with the previous studies (Randel et al., 2009; Diallo et al., 2018). From  
783 the present results, it is very clear that there is a significant decrease over the tropics and the  
784 increase over the mid-latitudes in 2015. These changes observed in the O<sub>3</sub> (decrease and increase)

785 are attributed due to the strengthening of the tropical upwelling and enhanced dowelling from the  
786 shallow branch of the Brewer-Dobson circulation in the mid-latitudes due to the strong El Niño  
787 conditions in 2015. Overall, it is concluded that initially, during July, the O<sub>3</sub> is transported into the  
788 anticyclone from the northeastern edges of the ASMA region through the sub-tropical westerlies  
789 and then it is isolated within the ASMA region. This is further supported by the southward  
790 meandering of the westerly jet and southward shift of the ASMA (negative GPH anomalies) over  
791 the same region in July (Fig. 3). Also, significant transport of mid-latitude dry air is clear from the  
792 Fig. 6. Thus, it is clear from the results that the stratosphere to troposphere transport and horizontal  
793 advection along with the subtropical jet caused the strong enhancement of the O<sub>3</sub> within the ASMA  
794 in 2015.

Formatted: Subscript

Formatted: Subscript

Formatted: Subscript

795 Distinct features are evident in the  $O_3$  changes between July and August. Also, the observed  
796 changes in the  $O_3$  are well correlated with the observed GPH anomalies in both months (Fig. 3).  
797 In July, the  $O_3$  shows a pronounced increase in the ASMA at all the pressure levels. This increase  
798 is quite significant over the northeastern edges of the ASMA and quite high at 100 hPa compared  
799 to 82 hPa and 121 hPa. A more than 40% increase is found at 100 hPa particularly over the  
800 northeastern edges of the ASMA in July. Even at 82 hPa and 121 hPa, significant enhancement in  
801 the  $O_3$  concentrations are evident over the northeastern edges of the ASMA during July. This  
802 enhancement is clearly matching with the  $O_3$  transport from higher latitudes which is shown in  
803 Fig. 6 on a weekly scale from ERA interim data. Overall in July, the  $O_3$  shows a prominent increase  
804 over the northeastern edges of the ASMA at all the mentioned pressure levels and strongly  
805 supported the stratosphere-troposphere transport over the same region. It can be noticed that the  
806 ASMA is strongly associated with troposphere-stratosphere transport as well as stratosphere-  
807 troposphere transport (Gamy and Randel, 2016; Fan et al., 2017). Also it is well reported that the  
808 northern parts of the ASMA is an active region for stratosphere-troposphere transport processes  
809 (Sprenger et al., 2003; Škerlak et al., 2014).

810 In August, the  $O_3$  shows quite different features compared to July. A strong increase in the  $O_3$   
811 is observed over the western and eastern edges of the ASMA at all the pressure levels. The increase  
812 is quite significant at 100 hPa and even at 121 hPa. And the observed increase is found 40%  
813 compared to the long-term mean at respective pressure levels. Even over the northeastern edges of  
814 the ASMA, the increase of  $O_3$  still appeared in August as observed in July. It is noted that in July  
815 and August 2015, strong El Niño conditions have existed. We can expect a strong downwelling of  
816 the shallow branch of Brewer-Dobson circulation in the mid-latitudes (Diallo et al., 2018).  
817 Enhanced tropical upwelling over the tropics and strengthening of the downwelling in the northern

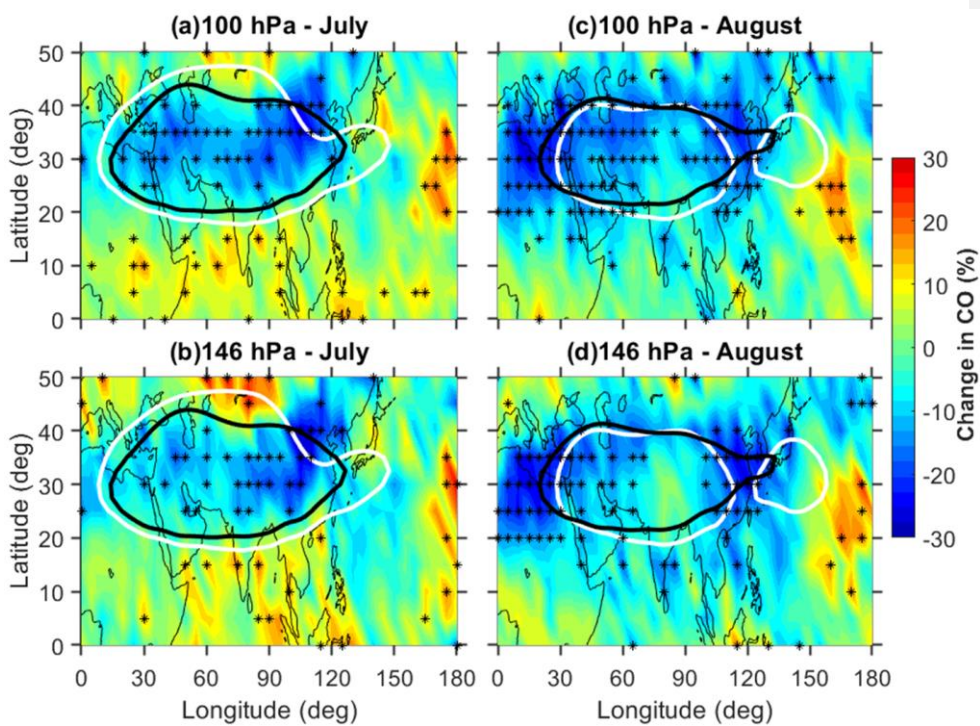
Formatted: Subscript

818 hemisphere mid-latitudes are likely to cause for the observed higher O<sub>3</sub> in the northern mid-  
819 latitudes during El Niño. Due to the enhanced tropical upwelling, stronger ozone transport from  
820 the tropics to the mid-latitudes is expected (Diallo et al., 2018). This clearly explains the observed  
821 high O<sub>3</sub> in the ASMA during 2015. Initially, during July, the O<sub>3</sub> is transported into the anticyclone  
822 from the northeastern edges of the ASMA region through the sub-tropical westerlies and then it is  
823 isolated within the ASMA region. This is further supported by the southward meandering of the  
824 westerly jet and southward shift of the ASMA (negative GPH anomalies) over the same region in  
825 July (Fig. 3). Also from the Fig. 6, very clear transport of mid-latitude dry air into the ASMA  
826 through the intrusions is seen. Thus, it is clear from the results that the stratosphere to troposphere  
827 transport of O<sub>3</sub> along with the subtropical jet caused the strong enhancement of the O<sub>3</sub> within the  
828 ASMA in July 2015. The confined O<sub>3</sub> within the anticyclone during July further separated from  
829 the anticyclone and transported to the tropics as well as to the extra-tropics over the western edges  
830 of the ASMA (~30°N) in August 2015.

831 **Fig-Figure 8a-b (Fig. 8c-d)** shows the spatial distribution of CO relative percentage change  
832 at 100 hPa and 146 hPa observed in during July (August) 2015. The white (black) color contour  
833 represents 16.75 km GPH at 100 hPa for the corresponding month in 2015 (climatological mean).  
834 The observed changes in the CO clearly exhibit quite distinct features between July and August as  
835 observed in the O<sub>3</sub>. A significant decrease (~30%) is noticed in the CO concentrations over most  
836 of the AMSA in July. The maximum decrease of CO is noticed over the northeastern edges of the  
837 ASMA, located ~ 30-45°N, 90-120°E region. Whereas in August, the decrease of CO is more  
838 concentrated over the east and western edges of the ASMA at both the pressure levels. Overall, the  
839 MLS observed CO was ~30% below average (percentage decrease) compared to the climatological  
840 monthly mean within the ASMA in July and edges of the ASMA in August 2015. It is noted that

Formatted: Subscript

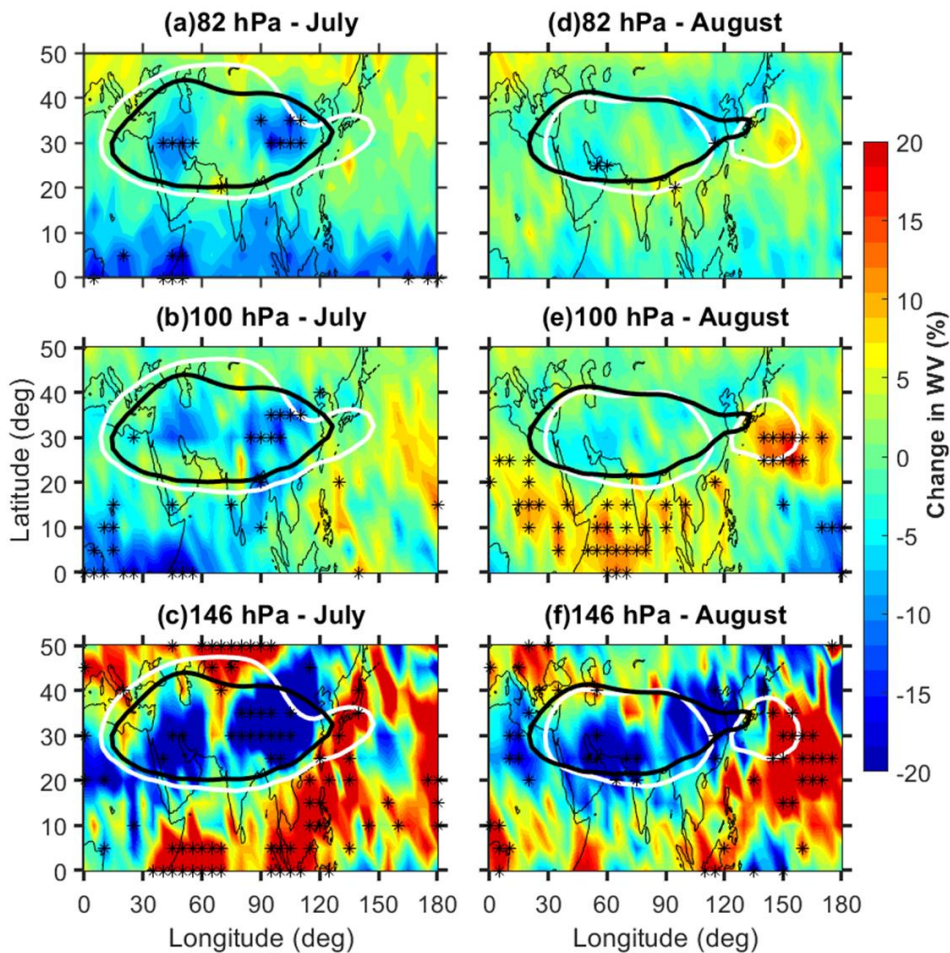
841 there is a considerable year-to-year variability of the CO sources over the ASM region (Santee et  
 842 al., 2017). The major sources of the CO over the ASM region are from the biomass burning and  
 843 industrial emission. The observed decreased CO within the ASMA in 2015 might be due to the  
 844 year-to-year variability in the CO sources and the weaker vertical transport due to the El Niño  
 845 conditions in 2015.



846 **Figure 8.** Carbon monoxide relative percentage change in-during July 2015 with respect to  
 847 climatological monthly mean observed at (a) 100 hPa and (b) 146 hPa. (c) and (d) same as (a) and  
 848 (b) but for the month of August. The white (black) color contour represents 16.75 km geopotential  
 849 height at 100 hPa for the corresponding month in 2015 (mean of 2005-2014). The star symbols  
 850 (black) shown in figure represent the anomalies greater than the  $\pm 2\sigma$  standard deviation of long-  
 851 term mean. The results are obtained from MLS measurements.

852 Similarly, the WV relative percentage change at 82 hPa, 100 hPa and 146 hPa in July (August)

854 2015 are shown in **Fig. 9a-b-c** (**Fig. 9e9d-df**). The WV shows quite different changes at ~~both all~~  
855 the pressure levels in July and August. At 146 hPa, the WV exhibits a strong decrease ( $> 20\%$ )  
856 within the ASMA in July as well as in August also. However, at 100 hPa and 82 hPa, the WV  
857 shows a relatively significant decrease within the ASMA in July compared to August. From the  
858 WV observations, it is concluded that the WV is strongly decreased at 146 hPa in both months.  
859 Whereas at 100 hPa and 82 hPa, the decrease in WV is quite high in July compared to August. It  
860 is also observed from the Fig. 9 that there is a significant enhancement of WV over the tropics at  
861 146 hPa in both months. But the WV enhancement is quite significant at 100 hPa, particularly  
862 during August compared to July. This enhancement in the WV around the tropical tropopause  
863 region in August is quite expected due to the El Niño conditions (Randel et al., 2009; Konopka et  
864 al., 2016). Overall, the tropospheric tracers (CO and WV) significantly decreased ( $\sim 30\%$  and  $20\%$ )  
865 within the ASMA during July and August 2015. These changes in the tropospheric tracers are  
866 might be due to the weaker vertical motions during the 2015 monsoon. A weaker vertical transport  
867 from the boundary layer to the UTLS is generally observed over the ASM region during El Niño  
868 period (Fadnavis et al., 2019). The El Niño conditions will suppress the monsoon convection and  
869 cause weaker vertical transport during monsoon. Also it is Well reported that the summer monsoon  
870 in 2015 was weaker monsoon due to the strongest El Niño conditions existed in 2015 (Tweedy et  
871 al., 2018; Yuan et al., 2019; Fadnavis et al., 2019). ~~These El Niño conditions will suppress the~~  
872 ~~monsoon convection and cause weaker vertical transport during monsoon.~~



873  
 874 **Figure 9.** Water vapour relative percentage change in July 2015 with respect to background  
 875 climatological monthly mean observed at (a) 82 hPa, (b) 100 hPa and (c) 146 hPa. (c) and (d) same  
 876 as (a) and (b) but for the month of August. The white (black) color contour represents 16.75 km  
 877 geopotential height at 100 hPa for the corresponding month in 2015 (mean of 2005-2014). The star  
 878 symbols (black) shown in figure represent the anomalies greater than the  $\pm 2\sigma$  standard deviation  
 879 of long-term mean. The results are obtained from MLS measurements.

880 From these results, it is clear that the enhancement of  $O_3$  and lowering of  $CO/WV$  is evident  
 881 in July and August 2015 compared to the climatological long-term monthly mean. The observed

882 high O<sub>3</sub> and low WV within the ASMA from the present study are consistent and well-matched  
883 with the previous study reported by Li et al. (2018). They demonstrated the importance of the  
884 large-scale atmospheric dynamics and the stratospheric intrusions for high O<sub>3</sub> and low WV over  
885 Lhasa within the ASMA by using in-situ balloon-borne measurements. The O<sub>3</sub>/WV changes  
886 strongly influence the background temperature structure within the UTLS region (Venkat Ratnam  
887 et al., 2016; RavindraBabu et al., 2019b). Further, we ~~tried to~~ investigated the tropopause  
888 temperature changes within the ASMA by using COSMIC RO data. The results are presented in  
889 the next following section.

### 890 3.3. Tropopause temperature anomalies in 2015

891 It is well known that the tropopause plays a crucial role in the exchange of WV, O<sub>3</sub> and other  
892 chemical species between the troposphere and the stratosphere. Most of these exchanges (WV to  
893 the lower stratosphere and O<sub>3</sub> to the upper troposphere) known as stratosphere troposphere  
894 exchange (STE) take place around the tropopause region (Fueglistaler et al., 2009; Venkat Ratnam  
895 et al., 2016; Ravindra Babu et al., 2019b). It is well reported that the tropopause within the ASMA  
896 is higher than the outside regions at the same latitude (Randel et al., 2010; Santee et al., 2017). It  
897 is a well known feature that the tropopause is higher over the ASMA than the surrounding regions  
898 (Randel et al., 2010; Santee et al., 2017). Also well documented that most of the STE processes  
899 that include WV and O<sub>3</sub> transport between troposphere and stratosphere are occur through the  
900 tropopause (Fueglistaler et al., 2009; Ratnam et al., 2016; Ravindra Babu et al., 2015, 2019b,  
901 2020). In the present study, we mainly focused on changes in the cold point tropopause temperature  
902 (CPT) and lapse rate tropopause temperature (LRT) within the ASMA in July and August 2015.  
903 The July and August 2015 monthly mean tropopause parameters are removed from the respective  
904 climatological monthly mean which is calculated by using COSMIC RO data from 2006 to 2014.

Formatted: Subscript

Formatted: Subscript

905 ~~One can note that we have strictly restricted our analysis within 40°N region for the cold point~~  
906 ~~tropopause. Kindly noticed that the analysis is strictly restricted within the 45° N region for the~~  
907 ~~cold point tropopause. Fig. Figure 10a-b (Fig. 10c-d) shows the CPT and LRT anomalies observed~~  
908 in July (August) 2015. The tropopause temperature anomalies (CPT/LRT) also exhibit a distinct  
909 pattern in July and August as observed in O<sub>3</sub> (Fig. 7). In July, the CPT/LRT anomalies show strong  
910 positive anomalies (~5 K) in most of the ASMA region. High positive CPT/LRT anomalies are  
911 also noticed over the ~~northwestern pacific (NWP)~~ region particularly below 20°N. These CPT/LRT  
912 anomalies observed over the NWP region ~~are~~ might be due to the El Niño induced changes in the  
913 Walker circulation and convective activity. Previous studies also observed significant warm  
914 tropopause temperature anomalies over WP and maritime continent during the El Niño period  
915 (~~Gettleman-Gettleman~~ et al., 2001). In August, the strong positive CPT/LRT anomalies (~5K) are  
916 concentrated over the northeastern edges of the anticyclone where the ~~western pacific WP~~ mode of  
917 the anticyclone ~~is was~~ separated from the ASMA. The temperature anomalies at 1 km above and  
918 below the CPH also show similar behavior as seen in the CPT/LRT during August 2015 (~~figures~~  
919 ~~not shown~~). Overall, the tropopause temperature anomalies in July and August 2015 within the  
920 ASMA are well correlated with the strong enhancement in the O<sub>3</sub> as shown in Fig. 7. However,  
921 the enhanced O<sub>3</sub> anomalies (heating due to the O<sub>3</sub>) itself cannot explain the observed positive  
922 tropopause temperature anomalies within the ASMA in 2015. This might be due to the El Niño  
923 induced changes in the convective activity and the circulation. It is well known that the reversal of  
924 walker circulation and the shifting of the convective activity (suppressed convective activity over  
925 ASM region) are generally observed during the warm phase of ENSO. One can be noticed that  
926 apart from the convection, other factors such as stratospheric QBO, atmospheric waves (gravity  
927 waves and Kelvin waves) also strongly influenced the tropopause temperatures. It is concluded

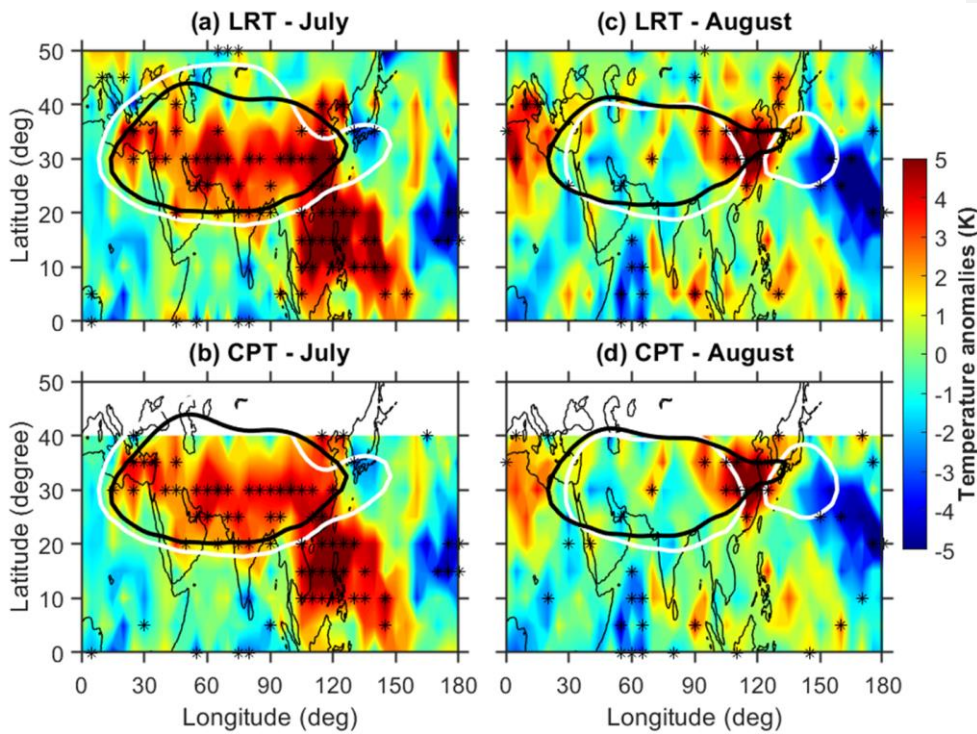
Formatted: Superscript

Formatted: Font: Not Bold

Formatted: Subscript

Formatted: Subscript

928 that the enhanced  $O_3$  within the ASMA is a main possible reason for the observed strong positive  
929 tropopause temperature anomalies in July and August 2015.



930  
931 **Figure 10.** Spatial distribution of (a) lapse rate tropopause temperature (LRT), (b) cold point  
932 tropopause temperature (CPT) anomalies in during July 2015. (c) and (d) same as (a) and (b) but  
933 for the month of August 2015. The white (black) color contour represents 16.75 km geopotential  
934 height at 100 hPa for the corresponding month in 2015 (mean of 2005-2014 climatological). The  
935 star symbols (black) shown in figure represent the anomalies greater than the  $\pm 2\sigma$  standard  
936 deviation of long-term mean.

#### 937 4. Summary and Conclusions

938 In this study, we investigated the detailed changes observed in the structure, dynamics and  
939 trace gases (Ozone, Water Vapor, Carbon Monoxide) variability within the ASMA in 2015 by using  
940 reanalysis products and satellite measurements observations. The tropopause temperature (CPT

941 and LRT) on monthly scales particularly during July and August 2015 also discussed. To quantify  
942 the changes that happened within the ASMA region, 11 years (2005-2015) of O<sub>3</sub>, WV and CO  
943 observations from the Aura-MLS data and 10 years (2006-2015) of tropopause temperature data  
944 from the COSMIC RO temperature profiles are used. The [NCEP-DOE Reanalysis 2](#) ~~NCEP~~  
945 ~~reanalysis~~ observed winds and GPH data from 2005 to 2015 are also utilized. The results are  
946 obtained by comparing the trace gas quantities in July and August 2015 with corresponding long-  
947 term monthly mean quantities.

948 The trace gases within the ASMA exhibit substantial anomalous behavior in July and August  
949 2015. During July and August 2015, we observed an enhancement of O<sub>3</sub> and the lowering of CO  
950 and WV over most of the ASMA region. The decrease of the tropospheric tracers (CO and WV) is  
951 quite expected due to the weaker upward motions from the weak monsoon ~~circulation~~ in 2015.  
952 This is supported by a recent study reported by Fadnavis et al. (2019). They showed weaker upward  
953 motions and deficient rainfall in the 2015 monsoon due to the strong El Niño conditions. However,  
954 the strong enhancement in the stratospheric tracer (O<sub>3</sub>) ~~ever~~ within the ASMA particularly over  
955 the northeastern edges of the ASMA during July is quite interesting. This is might be due to the  
956 stratospheric intrusions as well as transport from the mid-latitudes. Based on Fishman and Seiler  
957 (1983), it was stated that the positive correlation between CO and O<sub>3</sub> indicates, the O<sub>3</sub> is produced  
958 by in-situ in the troposphere whereas the correlation is negative means the O<sub>3</sub> originates from the  
959 stratosphere. We noticed a strong negative correlation between CO and O<sub>3</sub> in the present study  
960 with increased O<sub>3</sub> and decreased CO from the MLS measurements. This clearly reveals that the  
961 observed increased O<sub>3</sub> within the ASMA during 2015 is the stratospheric origin. This is further  
962 supported by higher negative GPH anomalies associated with a southward meandering of the  
963 subtropical westerly jet over northeastern Asia in July (**Fig. 3** and **4**). Further, the increased O<sub>3</sub> at

964 100 hPa and 121 hPa over western edges of the ASMA during August clearly indicates the transport  
965 of the O<sub>3</sub> towards outer regions through the outflow of the ASMA (**Fig. 7e-f**). Interestingly, the  
966 tropopause temperature obtained from the COSMIC RO data in July 2015 shows strong positive  
967 temperature anomalies (~5 K) over the entire ASMA region. These warm tropopause temperatures  
968 again supported the increased O<sub>3</sub> within the ASMA during 2015. The major findings obtained from  
969 the present study are summarized in the following.

970 ❖ The spatial extension of the ASMA region shows higher than long-term mean except over  
971 northeastern Asia where it exhibits a strong southward shift in July. Whereas in August, the  
972 AMSA further separated into two anticyclones and the western Pacific mode anticyclone is  
973 clearly evident in August.

974 ❖ The combination of Rossby wave breaking and pronounced southward meandering of  
975 subtropical westerlies play a crucial role on the dynamical and structural changes in the  
976 ASMA in 2015.

977 ❖ Strong enhancement in O<sub>3</sub> at 100 hPa (>40%) is clearly evident within the ASMA and  
978 particularly higher over the northeastern edges of the ASMA in July. The enhanced O<sub>3</sub> is  
979 strongly associated with a dominant southward meandering of the subtropical westerlies. In  
980 August, the increased O<sub>3</sub> is significantly located over the western edges of the ASMA. This  
981 clearly indicates the transport from the ASMA to the edges through its outflow.

982 ❖ A significant lowering of CO and WV within the ASMA is noticed during summer 2015. The  
983 lowering of WV is higher at 146 hPa than 100 hPa. 30% (20%) decrease in CO (WV) is  
984 observed within the ASMA in 2015. The decrease in the WV is higher at 146 hPa than 100  
985 hPa.

986 ❖ Significant positive tropopause temperature anomalies (~5 K) is observed in the entire ASMA  
987 region in July whereas, in August, the strong positive anomalies are concentrated over the  
988 northeastern side of the ASMA.

989 The changes in the O<sub>3</sub> concentrations (increase/decrease) within the ASMA are one of the possible  
990 mechanisms to strengthening/weakening of the ASMA (Braesicke et al., 2011). By using idealized  
991 climate model experiments, Braesicke et al. (2011) clearly demonstrated that the strengthening  
992 (weakening) of the ASMA occurred when the O<sub>3</sub> is decreased (increased) within the ASMA. The  
993 increased O<sub>3</sub> within the ASMA warms the entire anticyclone region and weakens the ASMA  
994 (Braesicke et al., 2011). Our results from the present study also in agreement with the results of  
995 Braesicke et al. (2011). We also observed a pronounced increase of O<sub>3</sub> within the ASMA associated  
996 with significant warming of tropopause as well as above and below the tropopause region in 2015.

997 By using precipitation index, wind data and stream functions, previous studies reported that the  
998 ASMA circulation in 2015 was weaker than the normal (Tweedy et al., 2018; Yuan et al.,  
999 20182019). Based on our present results, the strongly enhanced O<sub>3</sub> within the ASMA also might  
1000 be one of the plausible reasons for weakening of the ASMA in 2015. Based on our present results,  
1001 we conclude that the strong enhanced O<sub>3</sub> through the subtropical intrusions within the ASMA  
1002 region significantly warms around the tropopause region and caused an increase in the UTLS  
1003 temperature within the ASMA and indirectly leads to the weakening of the ASMA in 2015.

1004 **Author contributions:** SRB designed the study, conducted research, performed initial data  
1005 analysis and wrote the first manuscript draft. MVR, GB, SKP and NHL edited the first manuscript.  
1006 All authors edited the paper.

1007 **Data Availability:** All the data used in the present study is available freely from the respective  
1008 websites. The MLS trace gases data obtained from Earth Science Data website. The

1009 ~~[NCEP Reanalysis 2 data provided by the NOAA/OAR/ESRL PSL, Boulder, Colorado, USA, from](http://www.cpc.ncep.noaa.gov/products/wesley/reanalysis2/kana/reanl2-1.htm)~~  
1010 ~~[their web site \(http://www.cpc.ncep.noaa.gov/products/wesley/reanalysis2/kana/reanl2-1.htm\)](http://www.cpc.ncep.noaa.gov/products/wesley/reanalysis2/kana/reanl2-1.htm)~~  
1011 ~~NCEP/NCAR reanalysis data are available from NOAA website~~  
1012 ~~<https://www.esrl.noaa.gov/psd/data/gridded/data.ncep.reanalysis.pressure.html>~~. The COSMIC  
1013 data is available from COSMIC CDAAC website (<http://cdaac->  
1014 [www.cosmic.ucar.edu/cdaac/products.html](http://www.cosmic.ucar.edu/cdaac/products.html)).

1015 **Competing interests:** The authors declare that they have no conflict of interest.

1016 **Acknowledgments:** Aura MLS observations obtained from the GES DISC through their FTP site  
1017 (<https://mls.jpl.nasa.gov/index-eos-mls.php>) is highly acknowledged. We thank the COSMIC Data  
1018 Analysis and Archive Centre (CDAAC) for providing RO data used in the present study through  
1019 their FTP site (<http://cdaac-www.cosmic.ucar.edu/cdaac/products.html>). We also thank to  
1020 NCEP/NCAR reanalysis for providing geopotential and wind data. We thank ECMWF for  
1021 providing ERA interim reanalysis data.

## 1022 References

- 1023 Anthes, R., Bernhardt, P., Chen, Y., Cucurull, L., Dymond, K., Ector, D., Healy, S., Ho, S., Hunt,  
1024 D., Kuo, Y., Liu, H., Manning, K., McCormick, C., Meehan, T., Randel, W., Rocken, C.,  
1025 Schreiner, W., Sokolovskiy, S., Syndergaard, S., Thompson, D., Trenberth, K., Wee, T., Yen, N.,  
1026 and Zeng, Z.: The COSMIC/FORMOSAT-3 – Mission early results, B. Am. Meteorol. Soc., 89,  
1027 313–333, 2008.
- 1028 Avery, M. A., Davis, S. M., Rosenlof, K. H., Ye, H., Dessler, A. E., 2017. Large anomalies in lower  
1029 stratospheric water vapour and ice during the 2015–2016 El Niño, Nat. Geosci., 10, 405–409,  
1030 <https://doi.org/10.1038/ngeo2961>.
- 1031 ~~Barnston, A. G. and Livezey, R. E.: Classification, seasonality and persistence of low frequency~~  
1032 ~~atmospheric circulation patterns; Mon. Weather Rev. **115**(6) 1083–1126, 1987.~~
- 1033 Basha, G., Ratnam, M. V., and Kishore, P.: Asian Summer Monsoon Anticyclone: Trends and  
1034 Variability, Atmos. Chem. Phys. Discuss., <https://doi.org/10.5194/acp-2019-668>, in review,  
1035 2019.

1036 Bergman, J. W., Fierli, F., Jensen, E. J., Honomichl, S., and Pan, L. L.: Boundary layer sources for  
1037 the Asian anticyclone: Regional contributions to a vertical conduit, *J. Geophys. Res.-Atmos.*,  
1038 118, 2560–2575, <https://doi.org/10.1002/jgrd.50142>, 2013.

1039 Bian, J. C., Pan, L. L., Paulik, L., Vömel, H., and Chen, H. B.: In situ water vapor and ozone  
1040 measurements in Lhasa and Kunming during the Asian summer monsoon, *Geophys. Res. Lett.*,  
1041 39, L19808, <https://doi.org/10.1029/2012GL052996>, 2012.

1042 Braesicke, P., O. J. Smith, P. Telford, and J. A. Pyle (2011), Ozone concentration changes in the  
1043 Asian summer monsoon anticyclone and lower stratospheric water vapour: An idealised model  
1044 study, *Geophys. Res. Lett.*, 38, L03810, doi:10.1029/2010GL046228.

1045 Diallo, M., Riese, M., Birner, T., Konopka, P., Müller, R., Hegglin, M. I., Santee, M. L., Baldwin,  
1046 M., Legras, B., and Ploeger, F.: Response of stratospheric water vapor and ozone to the unusual  
1047 timing of El Niño and the QBO disruption in 2015–2016, *Atmos. Chem. Phys.*, 18, 13055–  
1048 13073, <https://doi.org/10.5194/acp-18-13055-2018>, 2018.

1049 Das, S.S., Suneeth, K.V., Ratnam, M.V., Girach, I. A., Das, S. K.: Upper tropospheric ozone  
1050 transport from the sub-tropics to tropics over the Indian region during Asian summer monsoon,  
1051 *Clim Dyn.*, 52: 4567. <https://doi.org/10.1007/s00382-018-4418-6>, 2019.

1052 Das, S., and Suneeth, K. V.: Seasonal and interannual variations of water vapor in the upper  
1053 troposphere and lower stratosphere over the Asian Summer Monsoon region- in perspective of  
1054 the tropopause and ocean-atmosphere interactions", *Journal of Atmospheric and Solar-*  
1055 *Terrestrial Physics* 201, 105244, doi:10.1016/j.jastp.2020.105244, 2020.

1056 Dessler, A. E., Schoeberl, M. R., Wang, T., Davis, S. M., Rosenlof, K. H., and Vernier, J. P.:  
1057 Variations of stratospheric water vapor over the past three decades, *J. Geophys. Res. Atmos.*,  
1058 119, 12 588–12 598, doi:10.1002/2014JD021712, 2014.

1059 Dunkerton, T. J.: The quasi-biennial oscillation of 2015–2016: Hiccup or death spiral?, *Geophys.*  
1060 *Res. Lett.*, 43, 10547–10552, <https://doi.org/10.1002/2016GL070921>, 2016.

1061 Fadnavis, S. and Chattopadhyay, R.: Linkages of subtropical stratospheric intraseasonal intrusions  
1062 with Indian summer monsoon deficit rainfall, *J. Climate*, 30, 5083–5095,  
1063 <https://doi.org/10.1175/JCLI-D-16-0463.1>, 2017.

1064 Fadnavis, S., Sabin, T.P., Roy, C. et al.: Elevated aerosol layer over South Asia worsens the Indian  
1065 droughts. *Sci Rep* 9, 10268, doi:10.1038/s41598-019-46704-9, 2019.

1066 Fan, Q., Bian, J. and Pan, L. L.: Stratospheric entry point for upper-tropospheric air within the  
1067 Asian summer monsoon anticyclone, *Sci. China Earth Sci.*, 60, 1685–  
1068 1693, <https://doi.org/10.1007/s11430-016-9073-5>, 2017.

1069 Fishman, J., and Seiler, W.: Correlative nature of ozone and carbon monoxide in the troposphere  
1070 - Implications for the tropospheric ozone budget; *J. Geophys. Res.* 88,  
1071 <https://doi.org/10.1029/JC088iC06p03662>, 1983.

1072 Fueglistaler, S., Dessler, A. E., Dunkerton, T. J., Folkins, I., Fu, Q., and Mote, P. W.: Tropical  
1073 Tropopause Layer, *Rev. Geophys.*, 47, G1004+, <https://doi.org/10.1029/2008RG000267>, 2009.

1074 Gadgil, S. and Francis, P. A.: El Niño and the Indian rainfall in June. *Curr Sci* 110:1010–1022,  
1075 2016.

1076 Garny, H. and Randel, W. J.: Transport pathways from the Asian monsoon anticyclone to the  
1077 stratosphere, *Atmos. Chem. Phys.*, 16, 2703–2718, [https://doi.org/10.5194/acp-16-2703-](https://doi.org/10.5194/acp-16-2703-2016) 2016,  
1078 2016.

1079 Gettelman, A., Randel, W. J., Massie, S., Wu, F.: El Niño as a natural experiment for studying the  
1080 tropical tropopause region, *J. Clim.*, 14, 3375– 3392, 2001.

1081 Gettelman, A., Kinnison, D. E., Dunkerton, T. J., and Brasseur, G. P.: Impact of monsoon  
1082 circulations on the upper troposphere and lower stratosphere, *J. Geophys. Res.-Atmos.*, 109,  
1083 D22101, <https://doi.org/10.1029/2004JD004878>, 2004.

1084 Highwood, E. J. and Hoskins, B. J.: The tropical tropopause, *Q. J. Roy. Meteor. Soc.*, 124, 1579–  
1085 1604, <https://doi.org/10.1002/qj.49712454911>, 1998.

1086 Ho, S.-P., Anthes, R. A., Ao, C.O., Healy, S., Horanyi, A., Hunt, D., Mannucci, A.J., Pedatella, N.,  
1087 Randel, W.J., Simmons, A., Steiner, A., Xie, F., Yue, X., Zeng., Z.: The  
1088 COSMIC/FORMOSAT-3 radio occultation mission after 12 years: Accomplishments,  
1089 remaining challenges, and potential impacts of COSMIC-2. *Bull Amer Met Soc* 100 online  
1090 version: <https://journals.ametsoc.org/doi/pdf/10.1175/BAMS-D-18-0290.1>

1091 Honomichl, S. B., and Pan, L. L.: Transport from the Asian summer monsoon anticyclone over the  
1092 western Pacific. *Journal of Geophysical Research: Atmospheres*, 125, e2019JD032094.  
1093 <https://doi.org/10.1029/2019JD032094>, 2020.

1094 Hossaini, R., Chipperfield, M., Montzka, M. P., Rap, S. A., Dhomse, S., and Feng, W.: Efficiency  
1095 of short-lived halogens at influencing climate through depletion of stratospheric ozone, *Nat.*  
1096 *Geosci.*, 8, 186–190. <https://doi.org/10.1038/ngeo2363>, 2015.

1097 ~~Jain, S., and Kar, S.C.: Transport of water vapour over the Tibetan Plateau as inferred from the~~  
1098 ~~model simulations. J. Atmos. Sol. Terr. Phys. 161, 64–75. [https://doi.org/](https://doi.org/10.1016/j.jastp.2017.06.016)~~  
1099 ~~[10.1016/j.jastp.2017.06.016](https://doi.org/10.1016/j.jastp.2017.06.016), 2017.~~

1100 Jiang, J.H., Su, H., Zhai, C., Wu, L., Minschwaner, K., Molod, A.M., Tompkins, A.M.: An  
1101 assessment of upper troposphere and lower stratosphere water vapor in MERRA, MERRA2,  
1102 and ECMWF reanalyses using Aura MLS observations. *J. Geophys. Res. Atmos.* 120, 11.  
1103 <https://doi.org/10.1002/2015JD023752>, 468–11,485, 2015.

1104 ~~[Kanamitsu, M., Ebisuzaki, W., Woollen, J., Yang, S.-K., Hnilo, J. J., Fiorino, M., and Potter, G. L.:](https://doi.org/10.1175/BAMS-83-11-1631)~~  
1105 ~~[NCEP-DOE AMIP-II Reanalysis \(R-2\), B. Am. Meteorol. Soc., 83, 1631–1643,](https://doi.org/10.1175/BAMS-83-11-1631)~~  
1106 ~~<https://doi.org/10.1175/BAMS-83-11-1631>, 2002.~~

1107 ~~Kalnay, E., Kanamitsu, M., Kistler, R., Collins, W., Deaven, D., Gandin, L., Iredell, M., Saha, S.,~~  
1108 ~~White, G., Woollen, J., Zhu, Y., Leetmaa, A., Reynolds, R., Chelliah, M., Ebisuzaki, W.,~~  
1109 ~~Higgins, W., Janowiak, J., Mo, K. C., Ropelewski, C., Wang, J., Jenne, R., and Joseph, D.: The~~  
1110 ~~NCEP/NCAR 40 year reanalysis project, B. Am. Meteorol. Soc., 77, 437–471, 1996.~~

1111 Khan, A., Jin, S.: Effect of gravity waves on the tropopause temperature, altitude and water vapor  
1112 in Tibet from COSMIC GPS Radio Occultation observations, *J. Atmos. Sol. Terr. Phys.* 138–  
1113 139, 23–31. <https://doi.org/10.1016/j.jastp.2015.12.001>, 2016.

1114 Kim, J. and Son, S.-W.: Tropical Cold-Point Tropopause: Climatology, Seasonal Cycle, and  
1115 Intraseasonal Variability Derived from COSMIC GPS Radio Occultation Measurements, *J.*  
1116 *Climate*, 25, 5343–5360, <https://doi.org/10.1175/JCLI-D-11-00554.1>, 2012.

1117 Kumar, K. K., Rajagopalan, B., Cane, M. A.: On the weakening relationship between the Indian  
1118 monsoon and ENSO. *Science* 287:2156–2159, 1999.

1119 ~~Kunze, M., Braesicke, P., Langematz, U., Stiller, G., Bekki, S., Brühl, C., Chipperfield, M.,~~  
1120 ~~Dameris, M., Garcia, R., and Giorgetta, M.: Influences of the Indian Summer Monsoon on~~  
1121 ~~Water Vapor and Ozone Concentrations in the UTLS as Simulated by Chemistry Climate~~  
1122 ~~Models, J. Climate, 23, 3525–3544, <https://doi.org/10.1175/2010jcli3280.1>, 2010.~~

1123 Kursinski, E. R., Hajj, G. A., Schofield, J. T., Linfield, R. P., and Hardy, K. R.: Observing Earth's  
1124 atmosphere with radio occultation measurements using the Global Positioning System, *J.*  
1125 *Geophys. Res.*, 102, 23429–23465, 1997.

1126 ~~[Konopka, P., Ploeger, F., Tao, M., and Riese, M.: Zonally resolved impact of ENSO on the](https://doi.org/10.1029/1997JD010819)~~  
1127 ~~[stratospheric circulation and water vapor entry values, J. Geophys. Res.-Atmos., 121, 11486–](https://doi.org/10.1029/1997JD010819)~~

1128 [11501, https://doi.org/10.1002/2015JD024698](https://doi.org/10.1002/2015JD024698), 2016.

1129 Li, Q., Jiang, J. H., Wu, D. L., Read, W. G., Livesey, N. J., Waters, J. W., Zhang, Y., Wang, B.,  
1130 Filipiak, M. J., Davis, C. P., Turquety, S., Wu, S., Park, R. J., Yantosca, R. M., and Jacob, D.  
1131 J.: Convective outflow of South Asian pollution: A global CTM simulation compared with EOS  
1132 MLS observations, *Geophys. Res. Lett.*, 32, L14 826, <https://doi.org/10.1029/2005GL022762>,  
1133 2005.

1134 ~~Li J, Yu R and Zhou T: Teleconnection between NAO and climate downstream of the Tibetan  
1135 Plateau; *J. Climate* 21(18), 4680–4690, 2008.~~

1136 ~~Li, D. and Bian, J.: Observation of a Summer Tropopause Fold by Ozone-sonde at Changchun,  
1137 China: Comparison with Reanalysis and Model Simulation, *Adv. Atmos. Sci.*, 32, 1354–1364,  
1138 <https://doi.org/10.1007/s00376-015-5022-x>, 2015.~~

1139 Li, D., Vogel, B., Müller, R., Bian, J., Günther, G., Li, Q., Zhang, J., Bai, Z., Vömel, H., and Riese,  
1140 M.: High tropospheric ozone in Lhasa within the Asian summer monsoon anticyclone in 2013:  
1141 influence of convective transport and stratospheric intrusions, *Atmospheric Chemistry and  
1142 Physics*, 18, 17 979–17 994, <https://doi.org/10.5194/acp-18-17979-2018>, [https://www.atmos-  
1143 chem-phys.net/18/17979/2018/](https://www.atmos-chem-phys.net/18/17979/2018/), 2018.

1144 ~~Lin, Z.D. and Lu, R. Y.: Inter annual meridional displacement of the East Asian upper tropospheric  
1145 jet stream in summer. *Advances in Atmospheric Sciences*, 22, 199–211, 2005.~~

1146 Livesey, N. J., Read, W. G., Wagner, P. A., Froidevaux, L., Lambert, A., Manney, G. L., Valle, L.  
1147 F. M., Pumphrey, H. C., Santee, M. L., Schwartz, M. J., Wang, S., Fuller, R. A., Jarnot, R. F.,  
1148 Knosp, B. W., and Martinez, E.: Version 4.2x Level 2 data quality and description document,  
1149 [https://mls.jpl.nasa.gov/data/v4-2\\_data\\_quality\\_document.pdf](https://mls.jpl.nasa.gov/data/v4-2_data_quality_document.pdf), 2018

1150 Nützel, M., Dameris, M., and Garmy, H.: Movement, drivers and bimodality of the South Asian  
1151 High, *Atmos. Chem. Phys.*, 16, 14755–14774, <https://doi.org/10.5194/acp-16-14755-2016>,  
1152 2016.

1153 Pan, L. L., Honomichl, S. B., Kinnison, D. E., Abalos, M., Randel, W. J., Bergman, J. W., and  
1154 Bian, J. C.: Transport of chemical tracers from the boundary layer to stratosphere associated  
1155 with the dynamics of the Asian summer monsoon, *J. Geophys. Res.-Atmos.*, 121, 14159–14174,  
1156 <https://doi.org/10.1002/2016JD025616>, 2016.

1157 Park, M., Randel, W. J., Kinnison, D. E., Garcia, R. R., and Choi, W.: Seasonal variation of  
1158 methane, water vapor, and nitrogen oxides near the tropopause: Satellite observations and

1159 model simulations, *J. Geophys. Res.-Atmos.*, 109, D03302,  
1160 <https://doi.org/10.1029/2003jd003706>, 2004.

1161 Park, M., Randel, W. J., Gettelman, A., Massie, S. T., and Jiang, J. H.: Transport above the Asian  
1162 summer monsoon anticyclone inferred from Aura MLS tracers, *J. Geophys. Res.*, 112, D16309,  
1163 doi:10.1029/2006JD008294, 2007.

1164 Park, M., Randel, W. J., Emmons, L. K., Bernath, P. F., Walker, K. A., and Boone, C. D.: Chemical  
1165 isolation in the Asian monsoon anticyclone observed in Atmospheric Chemistry Experiment  
1166 (ACE-FTS) data, *Atmos. Chem. Phys.*, 8, 757–764, <https://doi.org/10.5194/acp-8-757-2008>,  
1167 2008

1168 Park, M., Randel, W. J., Emmons, L. K., and Livesey, N. J.: Transport pathways of carbon  
1169 monoxide in the Asian summer monsoon diagnosed from Model of Ozone and Related Tracers  
1170 (MOZART), *J. Geophys. Res.*, 114, D08303, <https://doi.org/10.1029/2008JD010621>, 2009.

1171 Ramaswamy, C.: A preliminary study of the behavior of the Indian southwest monsoon in relation  
1172 to the westerly jet-stream. Special Palmen No. *Geophysica*, 6, pp. 455-476, 1958.

1173 Randel, W. J. and Park, M.: Deep convective influence on the Asian summer monsoon anticyclone  
1174 and associated tracer variability observed with Atmospheric Infrared Sounder (AIRS), *J.*  
1175 *Geophys. Res.*, 111, D12314, <https://doi.org/10.1029/2005jd006490>, 2006.

1176 ~~[Randel, W. J., Garcia, R. R., Calvo, N., and Marsh, D.: ENSO influence on zonal mean temperature  
1177 and ozone in the tropical lower stratosphere, \*Geophys. Res. Lett.\*, 36, L15822,  
1178 <https://doi.org/10.1029/2009GL039343>, 2009.](https://doi.org/10.1029/2009GL039343)~~

1179 ~~[Randel, W. J., Park, M., Emmons, L., Kinnison, D., Bernath, P., Walker, K. A., Boone, C., and  
1180 Pumphrey, H.: Asian monsoon transport of trace gases to the stratosphere, \*Science\*, 328, 611–  
1181 613, \[10.1126/science.1182274\]\(https://doi.org/10.1126/science.1182274\), 2010.](https://doi.org/10.1126/science.1182274)~~

1182 Randel, W. J., Park, M., Emmons, L., Kinnison, D., Bernath, P., Walker, K. A., Boone, C., and  
1183 Pumphrey, H.: Asian Monsoon Transport of Pollution to the Stratosphere, *Science*, 328, 611–  
1184 613, <https://doi.org/10.1126/science.1182274>, 2010.

1185 Rao, D.N., Ratnam, M.V., Mehta, S., Nath, D., Basha, G., Jagannadha Rao, V.V.M., et al:  
1186 Validation of the COSMIC radio occultation data over gadanki (13. 48°N, 79.2°E): A tropical  
1187 region, *Terr J Atmos Ocean Sci* 20, 59–70, [https://doi.org/10.3319/TAO.2008.01.23.01\(F3C\)](https://doi.org/10.3319/TAO.2008.01.23.01(F3C)),  
1188 2009.

- 1189 RavindraBabu, S., VenkatRatnam, M., Basha, G., Krishnamurthy, B. V., and Venkateswararao, B.:  
1190 Effect of tropical cyclones on the tropical tropopause parameters observed using COSMIC GPS  
1191 RO data, *Atmos. Chem. Phys.*, 15, 10239–10249, doi:10.5194/acp-15-10239-2015, 2015.
- 1192 RavindraBabu, S., VenkataRatnam, M., Basha, G., Liou, Y.-A., Narendra Reddy, N.: Large  
1193 Anomalies in the Tropical Upper Troposphere Lower Stratosphere (UTLS) Trace Gases  
1194 Observed during the Extreme 2015–16 El Niño Event by Using Satellite Measurements,  
1195 *Remote Sensing*, 2019, 11, 687. <https://doi.org/10.3390/rs11060687>, 2019. a
- 1196 RavindraBabu, S., Venkat Ratnam, M., Basha, G., Krishnamurthy, B.V.: Indian summer monsoon  
1197 onset signatures on the tropical tropopause layer. *Atmos. Sci. Lett.* 20, e884.  
1198 <https://doi.org/10.1002/asl.884>, 2019. b
- 1199 Ravindra Babu, S., Akhil Raj, S.T., Basha, G., Venkat Ratnam, M.: Recent trends in the UTLS  
1200 temperature and tropical tropopause parameters over tropical South Indian region, *J. Atmos.*  
1201 *Solar Terr. Phys.* 197:105164. <https://doi.org/10.1016/j.jastp.2019.105164>, 2020.
- 1202 [Ravindra Babu, S. and Liou, Y. A.: Tropical tropopause layer evolution during 2015–16 El Niño](https://doi.org/10.1016/j.jastp.2020.105507)  
1203 [event inferred from COSMIC RO measurements, \*J. Atmos. Solar Terr. Phys.\* 212: 105507.](https://doi.org/10.1016/j.jastp.2020.105507)  
1204 <https://doi.org/10.1016/j.jastp.2020.105507>
- 1205 Samanta, D., Dash, M. K., Goswami, B. N., and Pandey, P. C.: Extratropical anticyclonic Rossby  
1206 wave breaking and Indian summer monsoon failure. *Climate Dyn.*, 46, 1547–1562,  
1207 doi:<https://doi.org/10.1007/s00382-015-2661-7>, 2016.
- 1208 Santee, M. L., Manney, G. L., Livesey, N. J., Schwartz, M. J., Neu, J. L., and Read, W. G.: A  
1209 comprehensive overview of the climatological composition of the Asian summer monsoon  
1210 anticyclone based on 10 years of Aura Microwave Limb Sounder measurements, *J. Geophys.*  
1211 *Res.-Atmos.*, 122, 5491–5514, <https://doi.org/10.1002/2016jd026408>, 2017.
- 1212 Scherllin-Pirscher, B., Kirchengast, G., Steiner, A. K., Kuo, Y.-H., and Foelsche, U.: Quantifying  
1213 uncertainty in climatological fields from GPS radio occultation: an empirical-analytical error  
1214 model, *Atmos. Meas. Tech.*, 4, 2019–2034, doi:10.5194/amt-4-2019-2011, 2011a.
- 1215 Scherllin-Pirscher, B., Steiner, A. K., Kirchengast, G., Kuo, Y.-H., and Foelsche, U.: Empirical  
1216 analysis and modeling of errors of atmospheric profiles from GPS radio occultation, *Atmos.*  
1217 *Meas. Tech.*, 4, 1875–1890, doi:10.5194/amt-4-1875-2011, 2011b.
- 1218 [Shine, K. P. and Forster, P. M. D. F.: The effect of human activity on radiative forcing of climate](https://doi.org/10.1016/j.gloplacha.1999.02.001)  
1219 [change: a review of recent developments, \*Glob. Planet. Change\*, 20, 205–225, 1999.](https://doi.org/10.1016/j.gloplacha.1999.02.001)

1220 Song, Y., Lü, D., Li, Q., Bian, J., Wu, X., and Li, D.: The impact of cut-off lows on ozone in the  
1221 upper troposphere and lower stratosphere over Changchun from ozonesonde observations, *Adv.*  
1222 *Atmos. Sci.*, **33**, 135–150, <https://doi.org/10.1007/s00376-015-5054-2>, 2016.

1223 Sprenger, M., Maspoli, M. C., and Wernli, H.: Tropopause folds and cross-tropopause exchange:  
1224 A global investigation based upon ECMWF analyses for the time period March 2000 to  
1225 February 2001, *J. Geophys. Res.*, **108**, 8518, <https://doi.org/10.1029/2002JD002587>, 2003.

1226 Škerlak, B., Sprenger, M., and Wernli, H.: A global climatology of stratosphere–troposphere  
1227 exchange using the ERA-Interim data set from 1979 to 2011, *Atmos. Chem. Phys.*, **14**, 913–  
1228 937, <https://doi.org/10.5194/acp-14-913-2014>, 2014.

1229 Tweedy, O. V., Waugh, D. W., Randel, W. J., Abalos, M., Oman, L. D., and Kinnison, D. E.: The  
1230 Impact of Boreal Summer ENSO Events on Tropical Lower Stratospheric Ozone, *Journal of*  
1231 *Geophysical Research: Atmospheres*, **123**, 9843–9857, <https://doi.org/10.1029/2018JD029020>.

1232 Uppala, S. M., Kållberg, P. W., Simmons, A. J., Andrae, U., da Costa Bechtold, V., Fiorino, M.,  
1233 Gibson, J. K., Haseler, J., Hernandez, A., Kelly, G. A., Li, X., Onogi, K., Saarinen, S., Sokka,  
1234 N., Allan, R. P., Andersson, E., Arpe, K., Balmaseda, M. A., Beljaars, A. C. M., van de Berg,  
1235 L., Bidlot, J., Bormann, N., Caires, S., Chevallier, F., Dethof, A., Dragosavac, M., Fisher, M.,  
1236 Fuentes, M., Hagemann, S., Hólm, E., Hoskins, B. J., Isaksen, I., Janssen, P. A. E. M., Jenne,  
1237 R., McNally, A. P., Mahfouf, J. F., Morcrette, J. J., Rayner, N. A., Saunders, R. W., Simon, P.,  
1238 Sterl, A., Trenberth, K. E., Untch, A., Vasiljevic, D., Viterbo, P., and Woollen, J.: The ERA-40  
1239 re-analysis, *Q. J. Roy. Meteor. Soc.*, **131**, 2961–3012, <https://doi.org/10.1256/qj.04.176>, 2005.

1240 Vellore, R. K., Kaplan, M. L., and Krishnan, R., et al.: Monsoon-extratropical circulation  
1241 interactions in Himalayan extreme rainfall; *Clim. Dyn.* **46**, 3517, 2016.  
1242 <https://doi.org/10.1007/s00382-015-2784-x>.

1243 Venkat Ratnam, M., Ravindra Babu, S., Das, S. S., Basha, G., Krishnamurthy, B. V., and  
1244 Venkateswararao, B.: Effect of tropical cyclones on the stratosphere–troposphere exchange  
1245 observed using satellite observations over the north Indian Ocean, *Atmos. Chem. Phys.*, **16**,  
1246 8581–8591, <https://doi.org/10.5194/acp-16-8581-2016>, 2016.

1247 Vernier, J.-P., Thomason, L. W., and Kar, J.: CALIPSO detection of an Asian tropopause aerosol  
1248 layer, *Geophys. Res. Lett.*, **38**, L07804, <https://doi.org/10.1029/2010GL046614>, 2011

1249 Vernier, J.-P., Fairlie, T. D., Deshler, T., Ratnam, M. V., Gadhavi, H., Kumar, B. S., Natarajan,  
1250 M., Pandit, A. K., Raj, S. T. A., Kumar, A. H., Jayaraman, A., Singh, A. K., Rastogi, N., Sinha,

1251 P. R., Kumar, S., Tiwari, S., Wegner, T., Baker, N., Vignelles, D., Stenchikov, G., Shevchenko,  
1252 I., Smith, J., Bedka, K., Kesarkar, A., Singh, V., Bhate, J., Ravikiran, V., Rao, M. D.,  
1253 Ravindrababu, S., Patel, A., Vernier, H., Wienhold, F. G., Liu, H., Knepp, T. N., Thomason,  
1254 L., Crawford, J., Ziemba, L., Moore, J., Crumeyrolle, S., Williamson, M., Berthet, G., Jégou,  
1255 F., and Renard, J.-B.: BATAL: The balloon measurement campaigns of the Asian tropopause  
1256 aerosol layer, *B. Am. Meteorol. Soc.*, 99, 955–973, [https://doi.org/10.1175/BAMS-D-17-](https://doi.org/10.1175/BAMS-D-17-0014.1)  
1257 0014.1, 2018.

1258 Vogel, B., Günther, G., Müller, R., Groß, J.-U., Afchine, A., Bozem, H., Hoor, P., Krämer, M.,  
1259 Müller, S., Riese, M., Rolf, C., Spelten, N., Stiller, G. P., Ungermann, J., and Zahn, A.:  
1260 Longrange transport pathways of tropospheric source gases originating in Asia into the northern  
1261 lower stratosphere during the Asian monsoon season 2012, *Atmos. Chem. Phys.*, 16, 15301–  
1262 15325, <https://doi.org/10.5194/acp-16-15301-2016>, 2016.

1263 Wang, B., Xiang, B., Li, J., Webster, P. J., Rajeevan, M. N., Liu, J., Ha, K. –J.: Rethinking Indian  
1264 monsoon rainfall prediction in the context of recent global warming. *Nat Commun* 6:7154.  
1265 doi:10.1038/ncomms8154, 2015.

1266 Xu, X., Zhao, T., Lu, C., Guo, Y., Chen, B., Liu, R., Li, Y., Shi, X.: An important mechanism  
1267 sustaining the atmospheric “water tower” over the Tibetan Plateau. *Atmos. Chem. Phys.* 14,  
1268 11287–11295. <https://doi.org/10.5194/acp-14-11287-2014>.

1269 Yan, R.-C., Bian, J.-C., and Fan, Q.-J.: The Impact of the South Asia High Bimodality on the  
1270 Chemical Composition of the Upper Troposphere and Lower Stratosphere, *Atmos. Ocean. Sci.*  
1271 *Lett.*, 4, 229–234, 2011.

1272 Yan, R. C. and Bian, J. C.: Tracing the boundary layer sources of carbon monoxide in the Asian  
1273 summer monsoon anticyclone using WRF–Chem, *Adv. Atmos. Sci.*, 32, 943–951,  
1274 <https://doi.org/10.1007/s00376-014-4130-3>, 2015.

1275 Yan, X., Konopka, P., Ploeger, F., Tao, M., Müller, R., Santee, M. L., Bian, J., and Riese, M.: El  
1276 Niño Southern Oscillation influence on the Asian summer monsoon anticyclone, *Atmospheric*  
1277 *Chemistry and Physics*, pp. 8079–8096, <https://doi.org/10.5194/acp-18-8079-2018>, 2018.

1278 ~~Yang, S., Lau, K. M., Yoo, S. H., Kinter, J. L., Miyakoda, K. and Ho, C. H.: Upstream subtropical~~  
1279 ~~signals preceding the Asian summer monsoon circulation; *J. Climate*, 17, 4213–4229, 2004.~~

1280 Yu, P., Rosenlof, K. H., Liu, S., Telg, H., Thornberry, T. D., Rollins, A. W., Portmann, R. W., Bai,  
1281 Z., Ray, E. A., Duan, Y., Pan, L. L., Toon, O. B., Bian, J., and Gao, R.-S.: Efficient transport of

1282 tropospheric aerosol into the stratosphere via the Asian summer monsoon anticyclone,  
1283 Proceedings of the National Academy of Sciences, pp. 6972–6977,  
1284 <https://doi.org/10.1073/pnas.1701170114>, 2017.

1285 Yuan, C., Lau, W. K. M., Li, Z., and Cribb, M.: Relationship between Asian monsoon strength and  
1286 transport of surface aerosols to the Asian Tropopause Aerosol Layer (ATAL): interannual  
1287 variability and decadal changes, *Atmos. Chem. Phys.*, 19, 1901–1913,  
1288 <https://doi.org/10.5194/acp-19-1901-2019>, 2019.

1289 ~~Zhang, Q., Wu, G., and Qian, Y.: The Bimodality of the 100 hPa South Asia High and its~~  
1290 ~~Relationship to the Climate Anomaly over East Asia in Summer, *J. Meteorol. Soc. Jpn.*, 80,~~  
1291 ~~733–744, 2002.~~

1292 ~~Zheng, B., Chevallier, F., Ciais, P., Yin, Y., Deeter, M. N., Worden, H. M., Wang, Y., Zhang, Q.,~~  
1293 ~~and He, K.: Rapid decline in carbon monoxide emissions and export from East Asia between~~  
1294 ~~years 2005 and 2016, *Environ. Res. Lett.*, 13, 044007, [https://doi.org/10.1088/1748-](https://doi.org/10.1088/1748-9326/aab2b3)~~  
1295 ~~9326/aab2b3, 2018.~~

1296  
1297